Sampling the composition of cirrus ice residuals

Citation: Cziczo, Daniel J., and Karl D. Froyd. "Sampling the composition of cirrus ice residuals." Atmospheric Research 142 (1 June 2014), pp.15-31.

As Published: http://dx.doi.org/10.1016/j.atmosres.2013.06.012

Publisher: Elsevier

Persistent URL: http://hdl.handle.net/1721.1/105105

Version: Author's final manuscript: final author's manuscript post peer review, without publisher's formatting or copy editing

Abstract

Cirrus are high altitude clouds composed of ice crystals. They are the first tropospheric clouds that can scatter incoming solar radiation and the last which can trap outgoing terrestrial heat. Considering their extensive global coverage, estimated at between 25 and 33% of the Earth's surface, cirrus exert a measurable climate forcing. The global radiative influence depends on a number of properties including their altitude, ice crystal size and number density, and vertical extent. These properties in turn depend on the ability of upper tropospheric aerosol particles to initiate ice formation. Because aerosol populations, and therefore cirrus formation mechanisms, may change due to human activities, the sign of cirrus forcing (a net warming or cooling) due to anthropogenic effects is not universally agreed upon although most modeling studies suggest a positive effect. Cirrus also play a major role in the water cycle in the tropopause region, affecting not only redistribution in the troposphere but also the abundance of vapor entering the stratosphere. Both the current lack of understanding of cirrus properties and the need to improve our ability to project changes due to human activities in the future highlight the critical need to determine the aerosol particles on which cirrus form.

This review addresses what is currently known about the abundance, size and composition of cirrus-forming particles. We review aircraft-based field studies which have either collected cirrus ice residuals for off-line analysis or determined their size, composition and other properties in situ by capturing ice crystals and sublimating/removing the condensed phase water. This review is predominantly restricted to cirrus clouds. Limited comparisons are made to other ice-containing (e.g., mixed-phase) cloud types. The findings of recent reviews on laboratory measurements that mimic upper tropospheric cirrus formation are briefly summarized. The limitations of the current state of the art in cirrus ice residual studies are outlined. Important ancillary measurements and how they are integrated with ice residual data are also presented. Concluding statements focus on the need for specific instrumentation and future studies.

Contents

1. Introduction
2. Separation and characterization of cirrus ice residuals
    - 2.1 Separation
    - 2.2 Composition determination
3. Field studies
4. Ancillary measurements
    - 4.1 Cloud probes
    - 4.2 Relative humidity
5. Future studies
6. Concluding statements

Acknowledgements

References

Introduction

The definition of what is a cirrus cloud, and what is not, is complex. The classical definition of cloud type is based on morphology. According to the World Meteorological Organization [WMO, 1975] there are three morphologically different sub-types (genera) of high altitude clouds: 'cirrus' (detached clouds composed of filaments with a fibrous appearance), 'cirrocumulus' (thin sheets or layers) and 'cirrostratus' (semi-transparent fibrous with large sky coverage). The textbook *Cirrus* [2002], the most comprehensive recent review of this cloud type, expands on the morphological description and adds 'subvisible' or 'subvisual' cirrus (optical depth, normally considered at 0.694 micrometers wavelength, of < 0.03) and 'contrail cirrus' (due to input of water vapor from an aircraft). The properties of these clouds are summarized in Table 1. For the purpose of this review, cirrus are considered to be high altitude clouds of thin vertical extent composed predominately of ice crystals.

Regarding ice, *Cirrus* [2002] notes that "all cirrus clouds are composed of ice, but not all ice clouds are cirrus". Ice fogs and other glaciated near-surface clouds are not considered to be cirrus. Terrain induced ice clouds such as orographic or mountain wave clouds are often differentiated from cirrus because their formation mechanism couples them to the Earth's surface. Since they are occasionally grouped with the other cirrus types, they are briefly considered in this review. Of the cirrus types, only cirrocumulus and orographic can be mixed phase (containing ice and water droplets) whereas the remainder, apart from transient droplets or deliquesced aerosol particles during formation, are exclusively ice.

Cirrus are generally delineated by five different formation mechanisms (Figure 1). 'Synoptic cirrus' are formed by motion in the mid to upper troposphere, for example due to the jet stream or frontal passage. These clouds are induced by the cooling of rising air, normally in the range of few centimeters to a meter per second. Synoptic cirrus are believed to form on in situ aerosol particles and are observed to form from the top (i.e., the coldest point) and proceed downward as ice sediments [Starr and Cox, 1985]. 'Anvil' or 'injection cirrus' are formed by the high-altitude detrainment of ice from a cumulonimbus cloud. The formation of anvil cirrus is complex due to the uplift of aerosol particles, droplets and ice from the lower to upper troposphere, often at several meters per second. Ice formation competes with removal by sedimentation of the largest cloud elements – water droplets or ice crystals. Ice formation in anvil cirrus can take place on aerosol particles redistributed from the boundary layer or free tropospheric particles entrained within the convective system. 'Tropopause cirrus' are normally considered synonymous with the 'subvisible' type defined above. These clouds are restricted to the low temperatures observed at the high tropical tropopause (-70 - -90° C). Tropopause cirrus may be coupled to large scale vertical motions, for example from deep convection [Heymsfield, 1986] or gravity waves [Randel and Jensen, 2013]. 'Orographic' or 'wave clouds' are distinctly different from the remainder in that they are formed by meter per second or greater vertical motion imparted by terrain. These clouds are often mixed in phase and can form on aerosol particles from the boundary layer. 'Contrail cirrus' are the only purely anthropogenically formed cirrus, due to the input of water vapor in the mid to upper troposphere. Particles on which contrails form may be from the background free troposphere or due to the aircraft emissions. Contrails are composed of the highest

number and smallest size ice crystals of the cirrus types [Sassen 1997]. The formation mechanisms are shown schematically in Figure 1 and these naming conventions are used throughout this review. A more comprehensive description of various cirrus formation mechanisms is given in *Cirrus* [2002].

Cloud elements are understood to initially form on preexisting aerosol particles. These processes are shown schematically in Figure 2. For conditions above 0° C only liquid droplets can form. Considering the case of an uplifted and cooled air parcel, the water vapor in that parcel is expected to remain constant, but as it is cooled the relative humidity (RH) rises. If soluble aerosol particles are present those particles will rapidly take up water and grow significantly at their deliquescence point (e.g., ~80% in the case of sodium chloride or ammonium sulfate) [Seinfeld and Pandis, 2006]. These aqueous solution particles are often termed 'haze droplets' and may reach several micrometers in diameter. At a point slightly above 100% RH (i.e., slightly supersaturated with respect to liquid water), Koehler theory predicts that both haze droplets, insoluble aerosol particles, and internal mixtures will nucleate liquid water and grow, or 'activate', to super-micrometer cloud droplets [Seinfeld and Pandis, 2006]. Note that the initial aerosol particles can be soluble or insoluble or a combination of the two and either dissolve or remain immersed.

At temperatures below 0° C ice nucleation can occur once water vapor reaches saturation with respect to ice. Below this temperature liquid water has a higher vapor pressure than ice, increasingly so as temperature is further decreased. There are several known mechanisms by which particles can nucleate ice. The freezing mechanisms are grouped into two broad categories: heterogeneous (4+ known sub-mechanisms) and homogeneous freezing. Heterogeneous freezing occurs at higher temperatures and/or lower supersaturation with respect to ice and requires the action of a solid particle or inclusion, termed an 'ice nucleus' or IN [Pruppacher and Klett, 1997]. The known heterogeneous freezing mechanism are (1) immersion and condensation freezing, in which the IN nucleates ice from within a droplet, (2) contact freezing where a solid IN causes ice formation upon striking a droplet surface, and (3) deposition nucleation where water vapor directly forms ice upon a previously water-free IN surface. Immersion and condensation freezing are often considered to be synonymous but are distinguished by the separation of droplet formation and ice nucleation. In the case of immersion freezing the droplet is formed, possibly at temperatures warmer than 0° C, and ice nucleation occurs upon cooling. In the case of condensation nucleation the process of droplet activation occurs below 0° C and is immediately followed by ice nucleation [Pruppacher and Klett, 1997]. Several other heterogeneous ice nucleation mechanisms have been proposed but their atmospheric relevance is uncertain. These include 'inside out nucleation' where an immersed insoluble particle causes freezing upon impacting the droplet surface in a process similar to contact nucleation [Durant and Shaw, 2005]. Another mechanism is the "preconditioning" of an IN by a previous freezing event [Pruppacher and Klett, 1997; Kärcher and Lohmann, 2003]. Preconditioning assumes that in some cases ice will not fully evaporate from a particle surface despite subsaturated conditions. A particle which then experiences lower temperatures and/or supersaturation may freeze more readily than the original.

Heterogeneous freezing has been shown to depend on the size, surface composition and morphology of the IN [Pruppacher and Klett, 1997]. IN are rare in the background free

troposphere, with abundances from <1 to 100's per liter at temperatures greater than ~ -50° C [DeMott et al., 2003a]. A cirrus cloud which forms via heterogeneous mechanisms would therefore be expected to have no more than 100's of ice crystals per liter except in locations with abnormally abundant IN, such as in outflow regions of dust storms [DeMott et al., 2003b]. In the atmosphere this concentration can be modified by subsequent processes such as ice multiplication and removal by sedimentation.

Homogeneous freezing occurs when ice spontaneously forms within a solution, or haze, droplet. This process only occurs at temperatures below ~ -38° C for aerosol particles of diameter ~100 nm, the size typically found in the atmosphere, and at water vapor content near the saturation of liquid water (i.e., saturation ratio ~ 1.5 with respect to ice at -38° C). An aerosol particle which freezes homogeneously is termed a homogeneous freezing nucleus (HFN). The process of homogeneous freezing is better understood than heterogeneous freezing. Koop et al. [2000] showed that homogeneous freezing is a function of the particle volume and water activity (equivalent to RH for equilibrium conditions). Because given sufficient supersaturation all atmospheric particles can activate as droplets they can also act as HFN. Thus, unlike heterogeneous freezing, homogeneous freezing can result in 10^5 ice crystals or more per liter (i.e., up to the abundance of aerosol particles).

Figure 3 presents a diagram of condensation and freezing mechanisms in temperature versus supersaturation (with respect to ice) space. The various heterogeneous mechanisms are shown to occur at higher temperatures and/or lower supersaturation than homogeneous freezing. Note that droplet activation or deliquescence must occur before the immersion and condensation modes and both droplets and IN must be present to have contact freezing. Conversely, deposition nucleation can occur before liquid water saturation is reached. Only at the coldest temperatures and highest supersaturation does homogeneous freezing occur.

Two points are noteworthy. First, an ice crystal in a cirrus cloud is expected to contain either an IN or HFN. The known ice multiplication mechanisms, such as breakup of dendritic arms and the Hallet-Mossop process, act at temperatures significantly warmer than cirrus formation, which proceeds from -30 to -90° C [Hallett and Mossop, 1974]. Although possible mechanisms leading to ice multiplication in cirrus clouds have been proposed, at the time of this review there is no definitive evidence to support these theories [*Cirrus,* 2002]. Aggregation is not uncommon in some cirrus types such as frontal and anvil [Stith et al., 2011] although occurrence and quantification are difficult. Scavenging of particles by cirrus ice crystals has not been comprehensively addressed and, as described in the following sections, it can be confused with measurement artifacts. We proceed in the assumption of a single IN or HFN being present within each cirrus ice crystal. Second, the higher temperature portion of the cirrus formation regime is regarded by some authors as coinciding with the onset of homogeneous nucleation (i.e., ~ -38° C), but this is inconsistent with in situ and remote sensing observations which show cirrus formation at warmer temperatures [*Cirrus*, 2002]. The processes in Figure 3 therefore consider ice formation occurring at temperatures higher than the onset of homogeneous freezing. This is significant because, as indicated by the two hypothetical atmospheric trajectories in Figure 3, aerosol particles must first pass through one or more of the heterogeneous freezing regimes before encountering temperatures and water vapor conditions conducive to homogeneous freezing.

The implication that trajectories pass first through regions where heterogeneous ice nucleation mechanisms are active has been considered by researchers such as Kay et al. [2006] and Spichtinger and Cziczo [2010]. In brief, although the trajectories in Figure 3 initially pass through the heterogeneous regime, cirrus do not form exclusively by heterogeneous mechanisms. Instead, the combination of IN abundance and how rapidly a trajectory is traversed (i.e., the vertical velocity) determines where a cloud forms. For example, a high abundance of IN and a low vertical velocity will result in a heterogeneously formed cloud whereas a low abundance of IN and/or a rapid accent will result in homogeneously formed ice.

Direct observation of the aerosol freezing mechanism in the ambient atmosphere is difficult. However, the composition of residual particles within cirrus crystals can elucidate the formation mechanism. This has been demonstrated by DeMott et al. [2003a]. Using a continuous flow diffusion chamber (CFDC) which simulates the low temperature and high saturation conditions at which cirrus formed, DeMott et al. showed that HFN have a composition similar to the background free troposphere aerosol particles with a majority being internal mixtures of sulfate and organic carbon [Murphy et al., 1998]. Heterogeneously formed ice, conversely, is expected to have a residual composition consistent with that of IN. The study of DeMott et al. [2003a] showed IN to be predominantly mineral dust and metallic aerosol which is consistent with a compilation of studies by Pruppacher and Klett [1997].

2. Separation and characterization of cirrus ice residuals

The two critical steps in determination of the composition of cirrus ice residuals (IRs) are the separation of the ice crystals from the unactivated (interstitial) aerosol particles and subsequent (compositional) analysis. The distinction between IR and IN or HFN is that after nucleation an IN or HFN will acquire either gas- or particle-phase material via condensation or impaction scavenging. The residual material remaining after condensed phase water removal from a cirrus ice crystal is therefore termed an IR.

2.1 Separation

Counterflow virtual impaction is the most common technique used for separation of cloud elements from unactivated aerosol particles. First described by Ogren et al. [1985] for the separation of water droplets from aerosol particles in aircraft studies, a counterflow virtual impactor (CVI) inlet uses a flow of gas directed against the motion of the aircraft. This flow creates an inertial barrier which is a function of the aircraft velocity (i.e., particle velocity relative to the inlet) and counterflow rate. Shown schematically in Figure 4, the inertial barrier is adjusted to exclude aerosol particles but to allow more massive ice crystals to enter the inlet. The smallest size ice crystal which can pass the counterflow is termed the lower cutpoint or cutsize, typically taken at 50% impaction efficiency. Since the counterflow effectively replaces the air when the crystals are entrained, a warm and dry counterflow can be used to sublimate the ice while retaining the non-volatile material as a residual aerosol particle. The stream into which the ice crystals are entrained is termed the sample flow. A CVI inlet can “over-sample” or enhance droplets and ice crystal concentrations since the cloud elements in a large sampling volume are impacted into a relatively small sample flow. Enhancement factors

depend on the specific CVI design as well as aircraft flight conditions. CVI inlets have been used by a number of researchers for cirrus IR sampling [Noone et al., 1992; Ström and Heintzenberg, 1994; Heintzenberg, 1996; Ström et al. 1997; Petzold et al., 1998; Twohy and Gandrud, 1998; Seifert et al., 2003; Seifert et al., 2004; Cziczo et al, 2004a; Twohy and Poellot 2005; Pratt et al., 2009; Targino et al., 2010; Froyd et al., 2010; Stith et al., 2011; Cziczo et al., 2013] with results shown in the next section.

There are several fundamental limitations of CVI inlets. First, when used in cirrus clouds, CVI inlets need to operate at extremely high separation efficiency. The reason is that cirrus clouds can contain very low number densities of ice crystals, often <1 and, on average, only ~ 30 per liter [Cirrus, 2002; Randel and Jensen, 2013]. Because the background aerosol abundance can be 100 per cm^3, a rejection of $>10^4$-10^5 is required to ensure less than 1% of IRs are incorrectly transmitted aerosol particles. Using aircraft [Cziczo et al., 2004; Froyd et al., 2010] and a CVI designed for laboratory use [Boulter et al., 2005] this rejection factor has been shown to be possible. Pekour and Cziczo [2011] demonstrated that several mechanisms can lead to unintentional transmission of aerosol particles below the CVI cutpoint, including particles riding in the wake of large ice crystals. Stith et al. [2011] and Pekour and Cziczo [2011] also calculated that aerodynamic stress can lead to breakup of ice crystals as they encounter the counterflow. Complications in aircraft sampling can also lead to inadvertent aerosol particle transmission such as a CVI angle-of-attack that deviates from flow streamlines or sampling under turbulent conditions.

Second, sampled crystals must be slowed and sublimated in order to be analyzed for IR. Slowing of crystals is related to their stopping distance. Shown in Figure 5 for an initial velocity of 200 meters per second and a counterflow of 300 K air, the stopping distance increases from ~0.04 meters for a 10 micrometer diameter crystal to > 1 meter for a 100 micrometer crystal. A related calculation is the time required to remove condensed phase water, shown in Figure 5 for two inlet flow velocities. Crystals with a 100 micrometer initial diameter require > 4 meters to fully sublimate for a typical inlet velocity of 0.5 meters per second. Sublimation of large crystals is only accomplished using very low flow velocities, ~0.1 meters per second. However, with such long residence times crystals will gravitationally settle to the bottom of the inlet prior to sublimation. Increasing the CVI temperature beyond ~350 K has diminishing returns because the sublimation rate becomes diffusion-limited and losses of volatile components will occur. Since traditional CVI inlets are < 0.5 meters in length, ice crystals >50 micrometers diameter are the limit of what can be sampled without crystal impaction. This limit of stopping and sublimation is termed the upper cutpoint. Three representative cirrus ice crystal size distributions are shown in Figure 6. For all except tropical tropopause cirrus, the crystal number mode lies outside the range that can be stopped and sublimated by traditional inlets. An advanced CVI inlet utilizing neon as a counterflow due to its higher viscosity and thermal conductivity and a "folded" design stops and sublimates crystals up to ~70 micrometers diameter [Cziczo et al., 2013]. At the time of this review there are no CVI inlets that have an ability to analyze IR from larger ice crystals without crystal impaction artifacts. Artifacts are explained in more detail in the following paragraphs.

Third, all aircraft CVI inlets separate only based on inertia and do not differentiate ice from liquid water. Although a phase-separation inlet has been used for ground base application by Mertes et al. [2007], this technique is currently too large and operates at

velocities too slow for cirrus-sampling aircraft. This limitation is significant because IR can not be determined within mixed-phase clouds, which normally contain a greater number of droplets than ice, often by orders of magnitude [Seinfeld and Pandis, 2006].

There are significant artifacts generated by CVI inlets. IR particles collected using CVI inlets that do not employ an orthogonal (pickoff) sampling arrangement (see Fig. 4) are more suspect since cirrus crystals can undergo impaction prior to IR collection although these provide an accurately determination of total water. In this case two CVI inlets (with and without orthogonal pickoff) might be considered. Due to the large stopping distance shown in Figure 5, it is known that ice crystals do not follow gas flow lines and can impact surfaces with high velocity [Korolev et al., 2005]. Large ice crystals are also known to break up without encountering surfaces at the high Weber number associated with deceleration [Stith et al., 2011; Pekour and Cziczo et al., 2011]. These impaction events abrade aircraft and inlet surfaces and generate artifact particles that are of similar size to cirrus IR. Crystal impaction and artifact generation mechanisms are shown schematically in Figure 7. These processes take place (1) outside the inlet when ice crystal fragments are accepted into the sample flow, (2) when large crystals impact the back surface of the inlet and (3) on the inner CVI surface in cases with non-zero aircraft angle of attack or yaw. Impact-generated artifacts were initially identified using single particle mass spectrometry (SPMS; described in the next section) by Murphy et al. [2004]. The various generation mechanisms are summarized in the following paragraph and in Figure 8.

Examples of artifact particles generated via the different impaction mechanisms are shown in Figure 8. Impaction events not only generate particles of pure inlet or aircraft material (Fig 8, Panels A-C), but ice crystals can also capture small amounts of foreign material (Fig 8, Panel D). When water is removed from the crystal fragments the analyzed IR can be a mixture of a real IN and foreign material. The foreign material within these mixtures often comprises a small fraction of the IR mass (< 1-10%), and such minor artifact signatures can go undetected by many composition analyses. Internal mixtures of a real atmospheric particle with trace amounts of inlet artifact material, such as gold or stainless steel, are common in some SPMS studies. For some artifact generation mechanisms it is still possible to sample and analyze the real cirrus IRs. However, aerosol particles previously adsorbed onto inlet surfaces are resuspended during cirrus encounters and can be mistaken for IR [Murphy et al., 2004]. This artifact generation mechanism can further confound IR analysis and is demonstrated here to produce substantial artifact signals. In the Tropical Composition, Cloud and Climate Coupling (TC4) aircraft study, sea salt aerosol coated inlet and aircraft surfaces during marine boundary layer flight legs. These adsorbed particles were subsequently resuspended in heavy cirrus and were detected in the IR flow stream. These artifact particles were positively identified by trace metallic elements, not present in typical sea salt particles, that may have leached from the inlet surface as a result of sea salt corrosion (Figure 8, Panel E). These artifacts were strongly correlated with ice crystal size, as were stainless steel particles. Even when sampling cirrus with crystal mode sizes <100 micrometers diameter, the resuspended artifacts represented ~50% of particles collected in the sample flow. Surface adsorption efficiency is likely to depend on aerosol phase, composition and sampling environment. Consequently, sea salt aerosol collected in the marine boundary layer may represent a worst case scenario. However, solid particles

have been observed to undergo the surface adsorption / resuspension process as well [Murphy et al., 2004].

Supporting evidence of artifacts generated in ice clouds has also been provided using a conventional inlet operated within anvil cirrus with particles analyzed by electron microscopy (EM) [Kojima et al., 2004]. Kojima et al. detected abundant aluminum, silicon and zinc-containing particles, which were suggested to be paint chipped by ice crystals. More recently, Perring et al. [2013] used a single particle soot photometer (SP2) to describe a significant BC artifact when a traditional forward-facing inlet was used in cirrus clouds. Perring et al. recommend a new inlet design to allow for interstitial sampling and showed the significance of artifacts when impaction was not considered. These studies have led to modern CVI and traditional inlets being constructed with distinct design elements (i.e., flow patterns) and materials such as titanium or gold [Stith et al., 2011; Froyd et al., 2010].

2.2 Composition

Characterization of IRs has been accomplished using three methods. In the first cirrus sampling flights ice crystals were sublimated for counting and, in some cases, sizing [Noone et al., 1992; Ström and Heintzenberg, 1994; Heintzenberg, 1996; Ström et al. 1997; Seifert et al., 2003; Seifert et al., 2004]. In subsequent studies particles were impacted onto grids for off-line size and morphology analysis using EM coupled to several compositional analysis methods [Petzold et al., 1998; Twohy and Gandrud, 1998; Twohy and Poellot 2005; Targino et al., 2010; Cziczo et al., 2013]. Because this method uses simple inertial impaction it requires relatively little space, power and complexity.

Since the early 2000's SPMS has been used for real-time in situ analysis of aerosol particles. Most SMPS instruments focus particles using an aerodynamic inlet. Particles are detected and sized using scattered light as they pass through one or two laser beams set a fixed distance apart. A second laser, normally in the near UV, is fired to evaporate the particle and ionize the components. Ions are extracted into a single- or dual-polarity time-of-flight mass spectrometer. In this way a complete mass spectrum is generated for each detected particle. SPMS is considered a qualitative analysis method since detected signals depend on the quantity of components and the efficiency with which they are ionized. SPMS has been recently reviewed by Murphy [2007]. SMPS has become the more common technique for IR analysis since ~2004 [Cziczo et al, 2004ab; Pratt et al., 2009; Froyd et al., 2010; Cziczo et al., 2013].

3. Field Studies

Separation of cirrus ice crystals using counterflow virtual impaction with subsequent off- or on-line analysis has been conducted since 1989. At the date of this review there are ~18 papers, discussed chronologically in this section, which characterize cirrus residuals. There are several related instrument description papers, referenced in these works, that are not considered here. Single field missions are sometimes considered in multiple papers so the number of studies (13) is somewhat less than the total papers. We include papers from glaciated orographic but not mixed-phase clouds. A summary of the presented data is given in Table 2.

The initial use of counterflow virtual impaction of cirrus was by Noone et al. [1992]. This study, the international cirrus experiment (ICE), was conducted aboard the DLR Falcon during October, 1989 over northern Europe and the North Sea. Cirrus residual number density, using a condensation nucleus counter (CNC) and size distributions from 0.15 to 10 micrometers diameter, using an optical particle counter (OPC), were measured in situ and compared to ice water content. Composition of the residual material was not determined. The CVI had lower and upper cutpoints of 4 and ~55 micrometers diameter. The upper cutpoint was based upon comparative measurements to cloud probes; limitations of this method are discussed in the next section. Theoretical determination of the upper cutpoint for this CVI was somewhat lower, 12 - 20 micrometers. One flight in a prefrontal/synoptic cloud (which may not have been fully glaciated) and four flights in cirrostratus were described. The OPC results showed averages of 30 – 225 IR per liter with a mode size between 0.3 and 0.7 micrometers diameter. It was noted that the CPC count was most often considerably higher, suggesting a second mode of IR constituting ~80% of the total, in the size range below 0.15 micrometers diameter. This 'bi-modal' distribution was discussed in more detail for these flights by Ström et al. [1994]. The authors considered shatter when ice crystals larger than the upper cutpoint were encountered and demonstrated that this likely happened in two cases. The authors suggested that other cases of high number density correlated with smaller ice crystals. Ice crystal shatter, later quantified by Field et al. [2003], was not considered the dominant small-mode IR source.

The second use of a CVI in glaciated clouds was by Ström and Heintzenberg [1994]. Two cirrus sampling flights took place on January 13 and 14, 1992 over southern Germany and the Austrian Alps. This instrument package was the same as in Noone et al. [1992] and was also flown on the DLR Falcon although only CNC data were presented. The authors conducted a theoretical calculation of the upper CVI cutpoint with a value between 12 and 20 micrometers diameter and report a value of ~25 micrometers when a comparison to was made to two cloud probes that quantified ice crystals from 20 to 600 micrometers diameter. The authors did not report data for concentrations less than 20 per liter, below which point the cloud probe concentration was equal or larger than the CVI concentration. The authors inferred that below this concentration the CVI was subject to losses; they did not consider the possibility of cloud probe overcounting which was later reported by Field et al. [2003]. The CVI data were reported to >3000 per liter although this corresponded to cloud probe densities of only ~1-10 ice crystals per liter. The discrepancy of $>10^3$ was inferred to be due to ice crystals below the cloud probe size limit. Ice crystal shatter was not considered.

The first compositional measurements of cirrus IRs using a CVI were accomplished by Heintzenberg et al. [1996]. The residuals were collected during the January 13, 15, and 17 flights also considered by Ström and Heintzenberg [1994]. Residuals were only collected on the first flight and these were compared to interstitial aerosol collected during the second and outside cloud particles on the third. The IR data corresponded to a flight section with ~ 90 crystals per liter. Impacted residuals larger than 0.12 micrometers diameter were investigated with electron microscopy for size, morphology (long versus orthogonal axis) and elemental analysis by energy dispersive x-ray (EDX) analysis. 84 IR were analyzed, compared to 50 interstitial and 98 out of cloud. A median 1 micrometer diameter for the IR was reported and a compositions similar to mineral. The IR

composition was different than the mineral dust in the interstitial and out of cloud cases, however. Samples of Saharan dust and Mt. Pinatubo volcanic ash were analyzed by the authors for comparison. The IRs were found to have had a higher abundance of iron and less silicon and aluminum compared to the other samples. Pitting of the inlet, later considered by Murphy et al. [2004], was not considered as a particle source.

Ström et al. [1997] presented data from the DRL Falcon using the same instrumental package described above. Four flights were conducted over southern Germany and Austria during March, 1994. Number density and size distributions were presented from the CVI and an interstitial inlet on one of these flights, March 18, in a cloud with a temperature from -35 to -60 °C. Note that Perring et al. [2013] have recently demonstrated artifacts that can be associated with the use of traditional inlets attempting to measure interstitial aerosol within clouds; this was not considered by Ström et al. [1997]. IR number density ranged up to 14000 with a median of 2500 per liter. IR composition was not determined. Contrail sampling was intentionally excluded by removal of data at high interstitial number density. The IR mode size was found to be below 0.3 micrometers diameter, suggesting that homogeneous freezing of sulfate droplets had led to this cloud formation.

Petzold et al. [1998] determined composition of cirrus, including contrail IRs, using the instrumental package described by Heintzenberg et al. [1996]. Four flights over Germany and Austria aboard the DLR Falcon during mid-October, 1996 were considered. Of these 2 contrail and 2 cirrus encounters were compared to 3 interstitial cases. A total of 380 contrail IRs, 197 cirrus IRs and 36 interstitial aerosol particles were analyzed by impaction on filters with off-line scanning electron microscope (SEM) and EDX. Interstitial and residual particles were grouped into three size classes with the majority of all samples in the smallest, between 0.1 and 0.5 micrometers. Four classes of composition were considered (black carbon (BC), metallic, metallic and BC, and silicate) with the majority of interstitials and residuals being BC. There are several inconsistencies in this paper that need to be specifically noted. First, interstitial aerosol particles were observed to be 70 – 95%, by number, BC. This number is more than an order of magnitude higher than reported by modern measurements of BC [Bond et al., 2013] and likely were caused by the artifacts produced by in cloud sampling with traditional inlets later shown by Perring et al. [2013]. Second, the number density of IR particles on the filter samples in contrail and cirrus corresponded to 200 and 20 per liter. When compared to the CNC IR concentrations (10000 and ~2000 per liter) the filter-based IR concentration represents only 1 - 2%. This suggests that 98-99% of IRs were smaller than 0.1 micrometers. Third, the metallic category corresponded to particles with a composition of stainless steel. Although the CVI inlet was made of this material the authors consider these to be of aircraft engine origin. Described more fully in subsequent sections, it is likely that ice crystal shatter and artifact generation due to pitting of the CVI resulted in the large number of small IRs and stainless steel composition.

A CVI inlet was used by Ström and Ohlsson [1998] aboard the DLR Falcon during the AEROCONTRAIL (Formation Processes and Radiative properties of particles in aircraft wakes) experiment in October 1996 over southern Germany. The inlet and experimental package were similar to that discussed in the previous references although the upper cutpoint of the CVI was described as 60 micrometers diameter. Ice crystal number density was compared to interstitial aerosol and absorbing IR number density in contrails

and cirrus clouds located in dense air traffic corridors during 5 flights. The number of absorbing IR was determined by sending the CVI sample flow to a particle soot absorption photometer (PSAP). The authors reported higher ice crystal number density in areas with higher absorbing aerosol concentration and suggested this was linked to the presence of aircraft exhaust.

Twohy and Gandrud [1998] analyzed IR in two contrails, one generated by a Boeing 757 and the other produced by the sampling aircraft, the NASA DC-8. The two flights were part of the Subsonic Assessment: Contrail and Cloud Effects Special Study (SUCCESS) which took place in April and May, 1996 over the south- and northwestern USA. The lower cutpoint of the CVI was variable, from 5 – 14 micrometers diameter during this study. An upper cutpoint was not presented. Residual number density was counted with one CNC and after heating to 250 °C with a second CNC. The heated value corresponded to the "non-volatile" IRs (i.e., above the volatility temperature of sulfates and some organics). Both CNCs had a lower size limit of 20 nm and reported concentration values ranging up to 12000 per liter for the total IRs and 9000 per liter for the non-volatile IRs. Chemical composition was determined by collecting a portion of the CVI sample flow on a two-stage impactor fitted with EM grids for off-line analysis. Assuming a density of 1.8 grams per cm^3 (similar to sulfates) the collection range for the first stage was 0.10 to 0.42 and the second stage >0.42 micrometers aerodynamic diameter. A total of 76 particles from the 757 and 36 particles from the DC-8 were analyzed. Soot IR represented 5 – 25%, metallic aerosol (stainless steel and titanium) 11 – 12 % and minerals were 31 – 48%.

Measurements of IRs were compared to interstitial aerosol for the interhemispheric differences in cirrus properties from anthropogenic emissions (INCA) project by Seifert et al. [2003]. The study was conducted with the DLR Falcon during March and April, 2000 based in Punta Arenas, Chile (10 flights) and also during September and October, 2000 from Prestwick, Scotland (9 flights). The CVI inlet was the same as that described by Ström et al. [1997] with the addition of a size-resolving differential mobility analyzer (DMA), which scanned from 0.025 to 0.1 micrometers diameter, in addition to a CNC and OPC for IR analysis. In both the northern and southern hemisphere data the number mode size of the IRs was found to be bi-modal with a small mode of super-micrometer size and the dominant mode of less than 0.1 micrometers diameter. The fraction of nucleated particles was calculated by comparing the IR number to the sum of interstitial and IR particles. Nucleated fractions exhibited a relatively flat profile with respect to size and increased from <0.1% when less than 300 IR were counted per liter to >4% at >3000 per liter. Seifert et al. [2004] considered total IRs versus non-volatile IRs in a method similar to Twohy and Gandrud [1998] for this same set of flights. Particles were classified as volatile, semi-volatile and non-volatile based on presence when heated to 125°, from 125 to 250°, and above 250° C. Samples were further divided into a colder and warmer cloud temperature range delineated by -38 ° C. The non-volatile IR fraction was relatively invariant in the two cloud temperature regimes with 10 – 30% in the northern and 20 – 40% in the southern hemispheres. Few semi-volatile particles were found so that the volatile particles corresponded to the remainder. In this context, non-volatile particles were assumed to be possible IN whereas volatiles particles were considered possible HFN.

A SPMS was first used in combination with a CVI inlet by Cziczo et al. [2004a]. Cirrus of predominantly convective origin (cumulonimbus anvils) were sampled during 12 flights for the Cirrus Regional Study of Tropical Anvils and Cirrus Layers - Florida Area Cirrus Experiment (CRYSTAL-FACE) from the NASA WB-57 aircraft over Florida and the Gulf of Mexico during July, 2002. Two flights encountered a cross-Atlantic transported Saharan dust layer. The lower and upper CVI cutpoints for these flights was 5 and 22 micrometers diameter, respectively. IRs from 0.2 to 2 micrometers were sized and their composition determined on a particle by particle basis. The IR mode size was between 0.3 and 1 micrometer diameter with the larger values corresponding to the Saharan dust flights. Spectra were grouped into four categories (sulfate/organic/biomass burning, sea salt, mineral dust/fly ash and others). A comparison was made between particles in the vicinity of clouds, interstitial and IRs. Outside cloud (2126 particles) and interstitial (299 particles) were observed to be predominantly (>95%) sulfate/organic/biomass burning. On 11 of the 12 flights the IRs (211 particles) were predominantly (>60%) mineral dust/fly ash and sea salt. In the case of the two flights in the vicinity of Saharan dust the IRs were >60% mineral dust. One of the flights (127 IRs) was considered consistent with homogeneous nucleation because the IR composition was predominantly sulfate/organic/biomass burning. EC was less than 1% of the particles near clouds and in the interstitial particles and IRs. Cziczo et al. [2004b] considered the relative abundance of organic material in IRs versus the frozen fraction during CRYSTAL-FACE. Organics were shown to be essentially absent at low frozen fractions, implying that homogeneous freezing was more likely on pristine sulfate particles. This observation was supported by kinetic arguments made by Kärcher and Koop [2005].

Cziczo et al. [2004a] reported that a considerable fraction, in some cases >80% of IRs, were composed of stainless steel, the same material that composed the CVI inlet. All metallic particles, stainless steel or otherwise, were removed from this dataset. These artifact particles were considered by Murphy et al. [2004] who showed that impacts of ice crystals at aircraft velocity (>180 m/s) could ablate metal inlets and thereby introduce contaminant particles into the sample flow. The implications were two-fold: (1) studies using CVIs in cirrus needed to consider the production of metallic aerosol from ice crystal impaction and (2) ice crystals could potentially shatter and produce multiple small ice “shards”. While one of these shards could contain the original IN or a major fraction of an HFN, each shard, when evaporated, would leave behind a small residual core of any material acquired via scavenging during the cloud lifetime and some soluble material from the IN or HFN distributed through the ice crystal. Murphy et al. [2004] suggested that future CVI inlets be plated with compositionally distinct materials less prone to pitting.

A CVI inlet was also utilized by Twohy and Poellot [2005] during CRYSTAL-FACE from the University of North Dakota Citation aircraft. The CVI inlet cutpoints were not reported. IRs were collected on a two stage impactor with cutsizes of 0.07 - 0.38 and >0.38 micrometer diameter assuming 1.7 g cm^{-3} density particles. IR number density was inferred from the number on the grids to correspond to 30 – 300 per L. Approximately 50 particles were analyzed using SEM/EDX on 14 in cloud and 4 out of cloud samples for a total of 1115 IRs and 400 ambient particles. Particles were categorized as crustal, organic, soot, sulfate, industrial, salt, mixed and unknown. Salts were the largest category by number for both the small and large size samples, 30 – 40%. Crustal material was 10 –

18% while industrial (metallic) particles were 6 – 29%. Soot was 7 – 10%. Artifacts such as stainless steel were found to be <2% of the residual particles. Twohy and Poellot [2005] discussed their results in the context of cloud probe data, noting for the first time among the papers discussed in this section, that these probes often overcounted crystal number by an order of magnitude or more because of shatter on the aircraft of inlets [Field et al., 2003; Korolev and Isaac, 2005]. Twohy and Poellot [2005] showed that insoluble IRs, presumably heterogeneous IN, were more common at warmer cloud top temperatures than soluble, presumable HFN, IRs. Twohy and Poellot [2005] also noted that their result of salt abundance as an IR was inconsistent with the Fridlind et al. [2004] theory, which used suspect cloud probe data, that convective systems entrain considerable mid-tropospheric aerosol particles.

Orographic cirrus IRs were sampled during the INTeraction of Aerosol and Cold Clouds (INTACC) experiment in October, 1999 over Scandinavia by Targino et al. [2006]. A total of 5 flights of the British Met Office C-130 aircraft were made using the CVI described by Noone et al. [1992]. 609 particles were analyzed using SEM/EDX. Particles were grouped based on size (sub- and super-micrometer diameter) and categorized based on their elemental abundance. Targino et al. [2006] noted that cloud temperatures exceeded -35 °C and inferred that IRs were IN and not HFN. In total, 23.3% of the IRs were mineral dust, 6.7% sea salt, and 23.3% presumed to be organic carbon. A further 24.1% were iron. Targino et al. [2006] attempted to account for possible artifact particles by removing those that contained only stainless steel components (Fe, Cr, Ni). Using these criteria, ~3% of the particles were removed. However, as shown by Murphy et al. [2004], metal pitted from an inlet surface can be mixed with other materials. These include the IR from the ice crystal and material that had adhered to the inlet wall. Mixed stainless steel and other components, considered valid IRs and not artifacts, were ~7% of the particles analyzed by Targino et al. [2006].

Pratt et al. [2009] used a SPMS to investigate a single glaciated orographic cloud during November, 2007 over Wyoming during the Ice in Clouds Experiment Layer Clouds (ICE-L). This study was conducted aboard the NCAR C-130 and utilized a CVI with a lower cutpoint of 7 micrometers diameter similar to that used by Twohy and Poellot [2005]. A total of 46 IRs between 0.14 and 0.7 micrometers diameter were analyzed. Of these 23 were mineral, 2 soot, 4 salt, and 2 organic carbon. Mixed mineral and biological material, inferred from the presence of organic carbon, nitrogen and phosphate, was found on 15 particles.

Subvisible cirrus at the tropical tropopause were investigated by Froyd et al. [2010]. Due to their altitude these represent the coldest cirrus; assuming a vertical displacement of <1 km between formation and sampling Froyd et al. [2010] estimated a temperature range of -73 to -88 °C. The CVI used by Cziczo et al. [2004a], modified with gold plating, was used on board the NASA WB-57 During the Costa Rica Aura Validation Experiment (CRAVE) during January and February, 2006. A total of 127 IRs were compared to 873 interstitial aerosol particles. Comparison was also made to redesigned cloud probes less prone to overcounting from crystal shatter. Ice crystal number density was shown to be <50 per liter in these clouds, and most crystals were within the size sampling range of the CVI. The composition of the residuals was predominately submicron sulfate/organic mixtures and was chemically indistinguishable from out of cloud aerosol. Froyd et al. suggested heterogeneous ice nucleation by anhydrous salts [Abbatt et al., 2006] and/or

organic glasses [Murray et al., 2009] could be the formation mechanism. Froyd et al. [2010] also demonstrated that artifact particles were present in anvil cirrus from pitting of the aircraft (e.g. fiberglass), the inlet, and inlet materials mixed with ambient particles. The presence of gold and other materials on the same particle was used as definitive proof that mixed inlet and ambient particles could be produced as an artifact. Moreover, Froyd et al. [2010] cautioned that in many cases the inlet material was a minor spectral feature.

Mixed-phase and glaciating clouds from cold fronts and extratropical storms over the Pacific Ocean were investigated by Stith et al. [2011]. A total of 14 flights using the NCAR GV platform were conducted during April and May, 2007. A titanium CVI inlet was used for ice crystal separation. The lower cutsize was 5 micrometers diameter. The upper cutpoint was not specified but the authors noted that crystals larger than ~70 micrometers diameter were likely to break up due to aerodynamic stress. A total of 4108 residuals were analyzed using EM/EDX. Black carbon as an IR was considered in a separate publication for 7 of these flights by Baumgardner et al. [2008] using an SP2. Comparisons were made to the number and composition of IN provided by a CFDC. Stith et al. [2011] showed that particles with "high enough titanium levels to potentially be from the inlet" varied from ~2% of 0.1 – 0.3 micrometer diameter particles to as much as 31% of super-micrometer particles. Low titanium particles and other artifacts were not described. Both Baumgardner et al. [2008] and Stith et al. [2011] note that the signal from titanium artifacts produced an unknown signal in the SP2. Stith et al. showed, through comparison to the CFDC, that the convective nature of the storm may have led to multiple scavenged particles per initial IN and no specific IR numbers or fractions were given. Stith et al. [2011] also noted that although IR were enhanced in number density relative to a cloud probe the number of IN from the CFDC, located after the CVI, were not enhanced. Biomass burning was indicated as the major category of the nuclei and scavenged particles with minimal mineral dust. Baumgardner et al. [2008] similarly noted an inability to separate the IN from the scavenged BC but suggested a major role of scavenging by comparing the IRs to the near cloud aerosol particles. Stith et al. [2011] noted that the biomass burning particles analyzed were complicated in composition and may have contained mineral components.

Cziczo et al. [2013] compared data from the TC4 aircraft campaign conducted from San Jose, Costa Rica during July and August, 2007 using the NASA DC-8, the Mid-latitude Airborne Cirrus Properties Experiment (MACPEX) based in Houston, Texas during March and April, 2012 using the NASA WB-57, and the CRAVE campaign to the study of Cziczo et al. [2004a]. A combination of anvil and synoptic cirrus were sampled during these flights. The CVI inlet during TC4 was described by Twohy and Poellot [2005]. An advanced CVI using a Ne counterflow for increased viscosity and heat transfer, a longer stopping distance and an inline laser to sublimate water were used during MACPEX. A SPMS was used during all flights (1119 IR particles) and a comparison was made to SEM/EDX IR samples during MACPEX (433 particles). Cziczo et al. [2013] showed that that majority of IRs were mineral dust and metallic particles (61%) which were enhanced from near cloud abundance of 5%. Sulfates, organic and biomass burning particles were depleted compared to their near cloud abundance. Sea salt was a common IR during flights conducted over ocean (25%). The IR mode size using EM was between 0.3 and 0.5 micrometers diameter. A comparison to RH data showed that the supersaturation near

cirrus was similar to the value found for heterogeneous freezing (120 – 140%) in laboratory studies. Redesigned cloud probe data provided frequent values of < 200 ice crystals per liter. Only a single case of a cloud with IR composition consistent with homogeneous freezing (sulfate/organic) was found during MACPEX. Cziczo et al. [2013] also showed that EC and biological material were neither abundant in the near cloud aerosol or IR, contributing < 1%.

4. Ancillary Measurements

4.1 Cloud Probes

The techniques to count, size and determine the composition of cirrus IRs in the previous section have often been compared to other in situ measurements to provide information about the freezing mechanism and/or temporal and spatial changes in cloud formation properties. Among the ancillary techniques, the most common has been a comparison to cloud probes which count and size the ice crystals. A complete discussion of cloud probes is beyond the scope of this manuscript, but recent reviews such as Baumgardner et al. [2011] comprehensively discuss the capabilities and limitations of these instruments.

Cloud probe data has predominantly been used for two purposes. First, ice crystals number density has been compared to CVI sample flow IR number density [e.g. Noone et al., 1992; Ström and Heintzenberg, 1994; Heintzenberg, 1996; Ström et al. 1997; Seifert et al., 2003; Seifert et al., 2004, Stith et al., 2011]. In these studies the comparison was often used as evidence of a functional CVI, for example by showing that the IR number was equivalent to the portion of the ice crystal size range above the CVI lower cutpoint and smaller than the upper cutpoint. In some cases, however, the CVI cutpoints were changed from their calculated values to limits that corresponded to agreement with the cloud probe data. For example, Ström and Ohlsson [1998] suggested an upper cutpoint of 60 micrometers diameter, instead of a calculated value by Ström and Heintzenberg [1994] of 12 – 20 micrometers. Second, the number density of ice crystals has been used to infer the mechanism of freezing either directly [Heymsfield and Miloshevich, 1993] or via comparison to IR composition [Cziczo et al., 2013]. As stated in the Introduction, heterogeneous freezing has been shown to be consistent with ice crystals from <1 – 100's per liter whereas homogeneous freezing can occur on the majority of aerosol particles (i.e., 10's or more per cm^3). Thus, cases with less than 100 ice crystals per liter may correlate with heterogeneous freezing whereas higher number densities could suggest homogeneous freezing.

There are limits to both types of comparison. Regarding direct comparison to ice crystal number density from cloud probes, it is now known that prior to ~2008 ice probes often overcounted ice crystal number density by an order of magnitude or more. Shown initially by Field et al. [2003] and Korolev and Issac [2005], ice crystals can impact probe inlets resulting in shatter phenomena that can lead to multiple shards. This process, shown schematically in Figure 7, is analogous to the impacts that can take place on CVI tips or walls [Murphy et al., 2004]. More recent work by McFarquhar et al. [2007], Jensen et al. [2009], Korolev et al. [2011] and Lawson [2011] have shown that shatter is a complex function of aircraft speed, ice crystal size and number density. These authors show that although the effect of shattering impacts can be decreased by removal of multiple small coincident ice crystals via the so-called interarrival time method, this does

not remove all incidents of overcounting [Field et al., 2006]. Redesigned probes and inlets since ~2008 appear to have reduced this problem significantly [Randel and Jensen, 2013]. Regarding use of ice number density to infer freezing mechanism, Jensen et al. [2013] has shown that cloud evolution after formation can critically impact ice concentration. For example, a localized homogeneous freezing event can, through advection and sedimentation, create a larger area of lower ice crystal number density that might mimic heterogeneous freezing. Similarly, Spichtinger and Krämer [2012] have shown low ice crystal concentration can be replicated by homogeneous freezing simulations using small scale, short frequency updrafts. Both of these limitations suggest previous work should be treated with caution and highlights the need to consider the limitations of in situ cloud microphysical measurements in future nucleation studies.

4.2 Relative Humidity

Measurements of RH with respect to ice have also been compared to IR number density and composition to infer freezing mechanism. As stated in the Introduction, heterogeneous freezing initiates at lower ice supersaturation levels than does homogeneous freezing. A preponderance of ~120% RH observations in the cirrus formation region suggest that heterogeneous nucleation regulates water vapor, whereas observations at 150% and greater would suggest that heterogeneous nucleation is not significant and that homogeneous nucleation is regionally dominant. This correlation of out of cloud RH and freezing mechanism was suggested by Heymsfield et al. [1998] and Haag et al. [2003]. Correlation of ice crystal presence and RH were made by Krämer et al. [2009] and Luebke et al. [2012]. Although supersaturations higher than those required for homogeneous freezing have been observed in the upper troposphere [Peter et al., 2006] these are normally restricted to very low temperatures where RH measurement errors are known to be greatest. Cziczo et al. [2013] show a correlation of IR composition with near cloud RH measurements. In cases where IR composition was dominated by IN such as mineral dust and metallic particles, near cloud RH is rarely in excess of that required for heterogeneous freezing. Comparisons between near cloud RH and cirrus properties are limited, however, by the strong gradients in aerosol properties, uplift velocity, water vapor near cloud edge.

5. Future studies

One of the major limitations of in situ studies of cirrus IR and microphysical properties is that sampling usually takes place well after the onset of nucleation; a visible cloud is often a requirement to start sampling. This implies a time lag between nucleation and measurement. For this reason the specific conditions required for nucleation are rarely, if ever, measured in aircraft studies. An understanding of the nucleation onset conditions, specifically temperature and ice saturation ratio, has prompted laboratory or separate field studies under well controlled conditions. Cloud nucleation is simulated in the laboratory using quasi-adiabatic expansions of multi-m^3 volumes lasting 10's of minutes [Möhler et al., 2005; Möhler et al., 2006], by creating supersaturated conditions in liter-size CFDCs [Archuleta et al., 2005], and other techniques [Abbatt et al., 2006; Dymarska et al., 2006; Knopf and Koop, 2006; Kanji and Abbatt, 2008; Welti et al., 2009; Baustian et al., 2012]. A recent review of these data was conducted by Hoose and Möhler [2012].

Several field studies have also used CFDCs to determine the nucleation temperature and saturation ratio of atmospheric aerosols. When deployed in free tropospheric conditions, for example at mountaintop sites [DeMott et al., 2003a; Chou et al., 2012], the aerosol is assumed to be similar to those on which upper tropospheric cirrus form. Off-line analysis using EM [Ebert et al., 2010] and in situ use of SPMS [DeMott et al., 2003a] have characterized these IN. Chen et al. [1998] and DeMott et al. [2003b] used CFDCs from aircraft to nucleate ice on free tropospheric aerosol followed by collection and off-line EM analysis of the residual material.

The studies of Chen et al. and DeMott et al. represent a possible path forward in studies of cirrus IR, whereby ice nucleation conditions can be determined in situ in cloud-free air, avoiding crystal shatter artifacts, by collection and characterization of the ice-forming aerosol. Ideally, this technique could be combined with SPMS for on-line analysis, as was the case for the mountain-top study of DeMott et al. [2003].

The CVI and cloud probe measurement artifacts summarized here highlight the need for characterization of IR composition at the single particle level. Abrasion of inlet material by ice crystal impaction likely explains the high metallic fraction of IR reported before SPMS was used [Heintzenberg et al., 1996; Petzold et al., 1998; Twohy and Gandrud, 1998]. When shatter of ice crystals occurs it is likely that multiple small particles, below the detection limit of an SMPS or EM but within a CNC size limit, are formed after sublimation of water. This may explain the high IR number density and low average size shown by Ström and Heintzenberg [1994], Ström et al. [1997] and Seifert et al. [2003]. Gold-plated and titanium inlets are now in use which should create compositionally distinct artifacts [Stith et al., 2011; Froyd et al., 2010]. Extreme care should also be taken in clouds with ice crystal sizes far exceed the upper CVI cutpoint since impaction artifacts will be maximized. Future airborne studies should consider use of lower velocity platforms to reduce the speed of the ice crystal relative to the inlet.

From Table 2 it is noteworthy that very few flights characterizing cirrus IRs have been conducted, and consequently, our knowledge of IR size and composition is limited. Of these flights, the vast majority have occurred in the northern hemisphere, mainly over continental Europe and the USA. Only 10 flights have taken place in the southern hemisphere, all conducted during a single season during the INCA campaign aboard the DLR Falcon. IR composition was not determined in these flights. Future airborne studies of ice nucleation should target the southern hemisphere, where different aerosol concentrations and compositions are likely to promote different cirrus nucleation mechanisms.

6. Concluding statements

Residual particles from ice crystals in glaciated cirrus and orographic clouds have been characterized during 115 flights during 13 studies. An additional 9 flights in contrails and contrail cirrus have been reported. Only since 1992 has the composition of the residual material within these ice crystals been characterized, initially using EM and later with mass spectrometry on a single particle basis. The key findings of these studies are:

1. CVI inlets, the technique of choice for separation of IRs from interstitial aerosol, are prone to impaction artifacts and can only separate ice crystals smaller than ~75 micrometers diameter.

Recent advances in cloud size distribution measurements show that most cirrus contain ice crystals with a mode size of 75 micrometers and greater. This is above the upper cutpoint of all modern CVI inlets and means that, to date, studies have only sampled a fraction of the cirrus ice crystal size distribution. Since large ice crystals cannot be stopped inside CVI inlets their impaction onto surfaces leads to artifacts. Artifact generation is a strong function of crystal size, and thus, altitude. Cirrus below ~8 km altitude are particularly susceptible to impaction and effectively cannot be sampled for IR analysis in all but the most ideal conditions (e.g., during dissipation). CVI inlet design and sampling can help mitigate artifact contamination. Compositionally distinct (i.e. titanium and gold-plated) modern CVI inlets attempt to address impaction but studies before ~2004 were subject to unknown artifacts. It is worth noting that even with an ideal CVI configuration that employs pickoff sampling for IR analysis and with careful artifact removal, the analyzed IR originate preferentially from ice crystals at the smallest end of the size distribution, often well below the crystal mode size. If the most effective IN are preferentially located within the largest crystals of a developing cirrus cloud, our current knowledge of IR properties may be systematically skewed to exclude a particular class of IN.

Furthermore, a comprehensive study of particle scavenging by cirrus is lacking. One complicating factor is the differentiation of scavenged particles from impaction artifacts since the two may have similar composition. Future work in this area is needed including both theoretical and experimental studies.

2. Mineral dust has typically been found as the most abundant IR in cirrus forming regions. EC, biomass burning and biological particles are rare cirrus IR.

This conclusion spans the study areas, although these are predominantly in the northern hemisphere [Heintzenberg et al., 1996; Petzold et al., 1998; Cziczo et al., 2004a; Twohy and Poellot, 2005; Targino et al., 2006; Cziczo et al., 2013]. Mineral dust mixed with biological material acting as an IN was shown by Pratt et al. [2009] during a single orographic cloud encounter with a small sample set. Although biological material may be an important IN near the Earth's surface it is noteworthy that none of the other cirrus flights reported biological material using either EM or SPMS. 'Black' or 'elemental carbon' have been reported as a significant IR in contrail studies [Petzold et al., 1998; Ström and Ohlsson, 1998; Twohy and Gandrud, 1998]. EC and biomass burning particles were shown to be rare as cirrus IRs by Cziczo et al. [2004a], Twohy and Poellot [2005], Targino et al. [2006], Pratt et al. [2009], Froyd et al. [2010] and Cziczo et al. [2013], although Stith et al. [2011] found this to be the major category in glaciating clouds in the Pacific. Sea salt appears as a significant fraction of the IRs when studies were conducted over open ocean, especially when anvil (convective) cirrus were sampled [Cziczo et al., 2004a; Twohy and Poellot, 2005; Targino et al., 2006].

3. Subvisible cirrus are compositionally distinct.

Froyd et al. [2010] showed that tropical tropopause subvisible cirrus in one location were composed of low number densities of small ice crystals that formed on sulfate and organic aerosol. Froyd et al. suggested that heterogeneous nucleation on glassy aerosol [Murray et al., 2009] or anhydrous salts [Abbatt et al., 2006] were possible mechanisms. Recent laboratory studies [Murray et al., 2010; Koop et al., 2011] have shown that glass transition temperatures for organic aerosol species extend to typical mid-latitude cirrus formation conditions. Conversely, Spichtinger and Krämer [2012] have suggested that

homogeneous freezing due to small scale fluctuations of vertical velocity, temperature and RH could be responsible for homogeneous formation of subvisible cirrus.

4. The composition of cirrus IRs are consistent with predominantly heterogeneous ice formation.

Stith et al. [2011] suggested significant ice nucleation at temperatures above -30° C and Cziczo et al. [2013] showed IR composition consistent with homogeneous freezing in only 2 flights out of 36 cloud encounters. These recent findings are inconsistent with previous research that suggested homogeneous freezing was dominant (e.g. Heymsfield et al. [1986] and Fridlind et al. [2003]), but it is noteworthy that the older studies are based on data prior to ~2008 when cloud probes overcounted ice crystal number density [Field et al., 2003; Korolev and Issac, 2005; McFarquhar et al., 2007; Jensen et al., 2009; Korolev et al., 2011]. Recent data using redesigned cloud probes exhibit lower concentrations of ice crystals, often <200 per liter [Jensen et al., 2012; Randel and Jensen, 2013] and warrant reconsideration of these findings.

5. Anthropogenic particles represent a significant fraction of cirrus IR.

Since the utilization of compositionally distinct CVI inlets, metallic particles have been shown to be a significant fraction of IR [Twohy and Poellot, 2005; Cziczo et al., 2013]. Previous studies which may have been impacted by artifacts should not be completely discounted (e.g., Heintzenberg et al. [1996], Petzold et al. [1998] and Twohy and Gandrud [1998]) but reports of metallic IR need to be carefully considered. As a whole, these studies suggest a possible anthropogenic source of cirrus ice forming aerosol, an indirect effect on cloud properties that has not been previously considered in studies of climate change [Solomon, 2007].

Acknowledgements

We thank Dan Murphy and Eric Jensen for useful discussions. We also thank the air and ground crews of the research aircraft involved in data collection. This research was supported by the NASA Earth Science Division Atmospheric Composition program award number NNH11AQ58UI.

References

Abbatt, J. P. D., Benz, S., Cziczo, D. J., Kanji, Z., Lohmann, U. and Möhler, O., Solid ammonium sulfate aerosols as ice nuclei: A pathway for cirrus cloud formation, Science, 313, 1770–1773, 2006.

Archuleta, C. M., DeMott, P. J. and Kreidenweis, S. M., Ice nucleation by surrogates for atmospheric mineral dust and mineral dust/sulphate particles at cirrus temperatures Atmos. Chem. Phys., 5, 2617–2634, 2005.

Baumgardner, D., et al., Airborne instruments to measure atmospheric aerosol particles, clouds and radiation: A cook's tour of mature and emerging technology, Atmos. Res., doi:10.1016/j.atmosres.2011.06.021, 2011.

Baumgardner, D., Subramanian, R., Twohy, C., Stith, J. and Kok, G., Scavenging of black carbon by ice crystals over the northern Pacific, Geophy. Res. Lett., 35, L22815, 2008.

Baustian, K. J., Cziczo, D. J., Wise, M. E., Pratt, K. A., Kulkarni, G., Hallar, A. G. and Tolbert, M. A., Importance of aerosol composition, mixing state and morphology for depositional ice nucleation: A combined field and laboratory approach, J. Geophys. Res., 117, D06217, 2012.

Bond, T. C., et al., Bounding the role of BC in the climate system: A scientific assessment, in press at J. Geophys. Res., 2013.

Boulter, J. E., Cziczo, D. J., Middlebrook, A. M., Thomson, D. S. and Murphy, D. M., Design and performance of a pumped counterflow virtual impactor, Aero. Sci. Tech., 40, 969-979, 2006.

Chou, C., Stetzer, O., Weingartner, E., Jurányi, Z., Kanji, Z. A. and Lohmann, U., Ice nuclei properties within a Saharan dust event at the Jungfraujoch in the Swiss Alps, Atmos. Chem. Phys., 11, 4725-4738, 2011.

Cirrus, Lynch, D. K., Sassen, K., Starr, D. C., Stephens, G. Eds., Oxford Univ. Press, New York, NY, 2002.

Chen, Y., Kreidenweis, S. M., McInnes, L. M., Rogers, D. C. and DeMott, P. J., Single particle analyses of ice nucleating aerosol particles in the upper troposphere and lower stratosphere, Geophys. Res. Lett., 25, 1391– 1394, 1998.

Cziczo, D. J., Murphy, D. M., Hudson, P. K. and Thomson, D. S., Single particle measurements of the chemical composition of cirrus ice residue during CRYSTAL-FACE, J. Geophys. Res., 109, D04201, 2004a.

Cziczo, D. J. et al., Observations of organic species and atmospheric ice formation Geophys. Res. Lett., 31, L12116, 2004b.

Cziczo, D. J., Froyd, K. D., Hoose, C., Jensen, E. J., Diao, M., Zondlo, M. A., Smith, J. B., Twohy, C. H. and Murphy, D. M., Clarifying the dominant sources and mechanisms of cirrus cloud formation, submitted to Science, 2013.

Davis, S., D. Hlavka, E. Jensen, K. Rosenlof, Q. O. Yang, S. Schmidt, S. Borrmann, W. Frey, P. Lawson, H. Voemel, and T. P. Bui, In situ and lidar observations of tropopause subvisible cirrus clouds during TC4, J. Geophys. Res.-Atmos., 115, 2010.

DeMott, P. J., Cziczo, D. J., Prenni, A. J., Murphy, D. M., Kreidenweis, S. M., Thomson, D. S. and Borys, R., Measurements of the concentration and composition of nuclei for cirrus formation, Proc. Natl. Acad. Sci., 100, 14,655–14,660, 2003a.

DeMott, P. J., Sassen, K., Poellot, M. R., Baumgardner, D., Rogers, D. C., Brooks, S. D., Prenni, A. J. and Kreidenweis, S. M., African dust aerosol particles as atmospheric ice nuclei, Geophys. Res. Lett., 30, 1732-1735, 2003b.

DeMott, P. J., J. G. Hudson, U. Bundke, and G. C. Roberts, Cloud condensation and ice nuclei, Chapter 4.6 in Airborne Measurements –Methods and Instruments, Wiley, 2013.

Durant, A. J. and Shaw, R. A., Evaporation freezing by contact nucleation inside-out, Geophys. Res. Lett., 32, L20814, 2005.

Dymarska, M., Murray, B. J., Sun, L. M., Eastwood, M. L., Knopf, D. A. and Bertram, A. K., Deposition ice nucleation on soot at temperatures relevant for the lower troposphere, J. Geophys. Res. Atmos.,111, D04204, 2006.

Ebert, M., et al., Chemical composition and mixing-state of ice residuals sampled within mixed phase clouds, Atmos. Chem. Phys., 10, 23865–23894, 2010.

Field, P. R., Wood, R., Brown, P. R. A., Kaye, P. H., Hirst, E., Greenaway, R. and Smith, J. A., Ice particle interarrival times measured with a fast FSSP, J. Atmos. Oceanic Technol., 20, 249– 261, 2003.

Field, P. R., Heymsfield, A. J. and Bansemer, A., Shattering and particle interarrival times measured by optical array probes in ice clouds, J. Atmos. Oceanic Technol., 23, 1357–1371, 2006.

Froyd, K. D., Murphy, D. M., Lawson, P., Baumgardner, D. and Herman, R., Aerosol particles that form subvisible cirrus at the tropical tropopause, Atmos. Chem. Phys., 10, 209–218, 2010.

Fridlind, A. M., Ackerman, A. S. and Jensen, E. J., Evidence for the predominance of mid-tropospheric aerosol particles as subtropical anvil cloud nuclei, Science, 304, 718–

722, 2004.

Haag, W., Kärcher, B., Ström, J., Minikin, A., Lohmann, U., Ovarlez, J. and Stohl, A., Freezing thresholds and cirrus cloud formation mechanisms inferred from in situ measurements of relative humidity, Atmos. Chem. Phys. 3, 1791-1806, 2003.

Hallett, J. and Mossop, S. C., Production of secondary ice particles during the riming process, Nature, 249, 26-28, 1974.

Heintzenberg, J., Okada, K. and Ström, J., On the composition of non-volatile material in upper tropospheric aerosol particles and cirrus crystals, Atmos. Res., 41, 81– 88, 1996.

Heymsfield, A. J., Ice particles observed in a cirriform cloud at -83 °C and implications for polar stratospheric clouds, J. Atmos. Sci., 43, 851-855, 1986.

Heymsfield, A. J., Miloshevich L. M., Twohy, C., Sachse, G. and Oltmans, S., Upper-tropospheric relative humidity observations and implications for cirrus ice nucleation, Geophys. Res. Lett. 25, 1343-1346, 1998.

Hoose, C. and Möhler, O., Heterogeneous ice nucleation on atmospheric aerosols: a review of results from laboratory experiments, Atmos. Chem. Phys. 12, 9817-9854, 2012.

Jensen, E. J. Leonhard, P. and Lawson, P., Using statistical comparisons between simulations and observations to understand physical processes controlling midlatitude cirrus ice size distributions, paper presented at the 16th International Conference on Clouds and Precipitation, Leipzig, Germany, 2012.

Jensen ,E. J. et al., On the importance of small ice crystals in tropical anvil cirrus, Atmos. Chem. Phys. 9, 5519–5537, 2009.

Kanji, Z. A., Florea, O. and Abbatt, J. P. D., Ice formation via deposition nucleation on mineral dust and organics: dependence of onset relative humidity on total particulate surface areas, Environ. Res. Lett., 3, 025004, 2008.

Kay, J. E., Baker, M. and Hegg, D., Microphysical and dynamical controls on cirrus cloud optical depth distributions, J. Geophys. Res., 111, D24205, 2006.

Kärcher, B. and Koop, T., The role of organic aerosols in homogeneous ice formation, Atmos. Chem. Phys., 5, 703-714, 2005.

Kärcher, B. and Lohmann, U., A parameterization of cirrus cloud formation: Heterogeneous freezing, J. Geophys. Res., 108, 4402, 2003.

Knopf, D. A., and Koop, T., Heterogeneous nucleation of ice on surrogates of mineral dust, J. Geophys. Res., 111, D12201, 2006.

Kojima, T., Buseck, P. R., Wilson, J. C., Reeves, J. M. and Mahoney, M. J., Aerosol particles from tropical convective systems: Cloud tops and cirrus anvils, J. Geophys. Res., 109, D12201, 2004.

Korolev, A and Isaac, G. A., Shattering during sampling by OAPs and HVPS. Part I: Snow particles, J. Atmos. Oceanic Technol., 22, 528–542, 2005.

Korolev, A. et al., Small ice particle observations in tropospheric clouds: Fact or artifact?, Bull. Amer. Meteor. Soc., 92, 967–973, 2011.

Koop, T., Luo, B., Tsias, A. and Peter, T., Water activity as the determinant for homogeneous ice nucleation in aqueous solutions, Nature, 406, 611–614, 2000.

Koop, T., J. Bookhold, M. Shiraiwa, and U. Poschl, 2011. Glass transition and phase state of organic compounds: dependency on molecular properties and implications for secondary organic aerosols in the atmosphere, PCCP, 13(43), 19238-19255.

Krämer, M. et al., Ice supersaturations and cirrus cloud crystal numbers, Atmos. Chem. Phys. 9, 3505-3522, 2009.

Lawson, R. P., B. Pilson, B. Baker, Q. Mo, E. Jensen, L. Pfister, and P. Bui, Aircraft measurements of microphysical properties of subvisible cirrus in the tropical tropopause layer, Atmos. Chem. Phys., 8, 1609-1620, 2008.

Lawson, R. P., Effects of ice particles shattering on the 2D-S probe, Atmos. Meas. Tech., 4, 1361–1381, 2011.

Luebke A. E., Avallone, L. M., Schiller, C., Rolf, C. and Krämer, M., Ice water content of arctic, midlatitude, and tropical cirrus – Part 2: Extension of the database and new statistical analysis Atmos. Chem. Phys. Discuss., 12, 29443–29474, 2012.

McFarquhar, G. M., Um, J., Freer, M., Baumgardner, D., Kok, G. L. and Mace, G., The importance of small ice crystals to cirrus properties: Observations from the Tropical Warm Pool International cloud Experiment (TWP-ICE), Geophys. Res. Lett. 57, L13803, 2007.

Mertes, S., et al., Counterflow virtual impactor based collection of small ice particles in mixed phase clouds for the physico-chemical characterization of tropospheric ice nuclei: Sampler description and first case study, Aero. Sci. Tech., 41, 848–864, 2007.

Möhler, O. et al., Effect of sulfuric acid coating on heterogeneous ice nucleation by soot aerosol particles, J. Geophys. Res. 110, D11210, 2005.

Möhler, O. et al., Efficiency of the deposition mode ice nucleation on mineral dust particles, Atmos. Chem. Phys., 6, 3007-3017, 2006.

Murphy, D. M. et al., Particle generation and resuspension in aircraft inlets when flying in clouds, Aero. Sci. Tech., 38, 401–409, 2004.

Murphy, D. M., Thomson, D. S. and Mahoney, M. J., In situ measurements of organics, meteoritic material, mercury, and other elements in aerosol particles at 5 to 19 kilometers, Science, 282, 1664–1669, 1998.

Murray, B. J., Wilson, T. W., Dobbie, S., Cui, Z., Möhler, O., Schnaiter, M., Wagner, R., Benz, S., Niemand, M., Saathoff, H., Ebert, V., Wagner, S., and Karcher, B., Glassy aerosols modify tropical tropopause cirrus and humidity, Nat. Geosci., 3, 233-236, 2009.

Murray, B. J., T. W. Wilson, S. Dobbie, Z. Cui, S. M. R. K. Al-Jumur, O. Mohler, M. Schnaiter, R. Wagner, S. Benz, M. Niemand, H. Saathoff, V. Ebert, S. Wagner, and B. Karcher, 2010. Heterogeneous nucleation of ice particles on glassy aerosols under cirrus conditions, Nature Geosci, 3, 233-237.

Ogren, J. A., Heintzenberg, J. and Charlson, R. J., In situ sampling of clouds with a droplet to aerosol particles converter, Geophys. Res. Lett., 12, 121–124, 1985.

Pekour, M. and Cziczo, D. J., Wake capture, particle breakup and other artifacts associated with counterflow virtual impaction, Aero. Sci. Tech., 45, 748-758, 2011.

Perring, A. E., Schwarz, J. P., Gao, R.S., Heymsfeld, A. J., Schmitt, C.G., Schnaiter, M., and Fahey, D. W., Evaluation of a perpendicular inlet for airborne sampling of interstitial submicron aerosol, submitted to Aero. Sci. Tech., 2013.

Peter, T., Marcolli, C., Spichtinger, P., Corti, T., Baker, M. B. and Koop, T., When dry air is too humid, Science, 1399-1402, 2006.

Petzold, A., Ström, J., Ohlsson, S. and Schroder, F. P., Elemental composition and morphology of ice-crystal residual particles in cirrus clouds and contrails, Atmos. Res., 49, 21– 34, 1998.

Pratt, K. A., DeMott, P. J., French, J. R., Wang, Z., Westphal, D. L., Heymsfield, A. J., Twohy, C. H., Prenni, A. J. and Prather, K. A., In situ detection of biological particles in cloud ice-crystals, Nat. Geosci., 2, 398–401, 2009.

Pruppacher, H. R., and Klett, J. D., Microphysics of Clouds and Precipitation, 2nd ed., D. Reidel, Norwell, Mass., 1997.

Randel, W. J. and Jensen, E. J., Physical processes in the tropical tropopause layer and their roles in a changing climate, Nat. Geosci., 6, 169-172, 2013.

Sassen, K., Contrail-cirrus and their potential for regional climate change, Bull. Amer. Meteor. Soc., 78, 1885-1904, 1997.

Seinfeld, J. H., and Pandis, S. N., Atmospheric Chemistry and Physics, 2nd ed., John Wiley & Sons, Inc., 2006.

Seifert, M., Ström, J., Krejci, R., Minikin, A., Petzold, A., Gayet, J.-F., Schumann, U., and Olvarlez, J., In situ observations of aerosol particles remaining from evaporated cirrus crystals: Comparing clean and polluted air masses, Atmos. Chem. Phys., 3, 1037-1049, 2003.

Seifert, M., Ström, J., Krejci, R., Minikin, A., Petzold, A., Gayet, J.-F., Schlager, H., Ziereis, H., Schumann, U. and Olvarlez, J., Thermal stability analysis of particles incorporated in cirrus crystals and of nonactivated particles in between the cirrus crystals: Comparing clean and polluted air masses, Atmos. Chem. Phys., 3, 3659-3679, 2004.

Solomon, S. ed., Climate Change 2007: The Physical Science Basis. Contribution of Working Group I to the Fourth Assessment Report of the IPCC, Cambridge Univ. Press, 2007.

Spichtinger, P., and Cziczo, D. J., Impact of heterogeneous ice nuclei on homogeneous freezing events, J. Geophys. Res., 15, D14208, 2010.

Spichtinger, P. and Krämer, M. Tropical tropopause ice clouds: A dynamic approach to the mystery of low crystal numbers Atmos. Chem. Phys. Discuss., 12, 28109-28153, 2012.

Starr, D. O'C., and Cox, S. K., Cirrus clouds. Part II: Numerical experiments on the formation and maintenance of cirrus, J. Atmos. Sci., 42, 2682-2694, 1985.

Stith, J. L., Twohy, C. H., DeMott, P. J., Baumgardner, D., Campos, T., Gao, R. and Anderson, J., Observations of ice nuclei and heterogeneous freezing in a Western Pacific extratropical storm, Atmos. Chem. Phys., 11, 6229-6243, 2011.

Ström, J. and Heintzenberg, J. Water vapor, condensed water and crystal concentration in orographically influenced cirrus clouds, J. Atmos. Sci., 51, 2368–2383, 1994.

Ström, J., Heintzenberg, J., Noone, K.J., Noone, K.B, Ogren, J.A., Albers, F. and Quante, M., Small crystals in cirriform clouds: A case study of residue size distribution, cloud water content and related cloud properties, J. Atmos. Res., 32, 125-141, 1994.

Ström, J., Strauss, B., Anderson, T., Schröder, J., Heintzenberg, J., and Wendling, P., In situ observations of the microphysical properties of young cirrus clouds, J. Atmos. Sci., 54, 2542–2553, 1997.

Ström, J., and Ohlsson, S., In situ measurements of enhanced crystal number densities in cirrus clouds caused by aircraft exhaust, J. Geophys. Res., 103, 11,355-11,361, 1998.

Targino, A. C., Krejci, R., Noone, K. J., and Glantz, P., Single particle analysis of ice

crystal residuals observed in orographic wave clouds over Scandinavia during INTACC experiment, Atmos. Chem. Phys., 6, 1977–1990, 2006.

Twohy, C. H., and Gandrud, B. W., Electron microscope analysis of residual particles from aircraft contrails, Geophys. Res. Lett., 25, 1359– 1362, 1998.

Twohy, C. H. and Poellot, M. R., Chemical characteristics of ice residual nuclei in anvil cirrus clouds: implications for ice formation processes, Atmos. Chem. Phys. **5**, 2289 2297, 2005.

Welti, A., et al., Influence of particle size on the ice nucleating ability of mineral dusts, Atmos. Chem. Phys., 9, 6705–6715, 2009.

World Meteorological Organization, International Cloud Atlas Vol. I, 407, Geneva, Switzerland, 1975.

Table and Figure Captions

Table 1. Mean and the range of cirrus cloud properties.

Table 2. Locations, timing, aircraft, number of flights and numbers of IRs analyzed for published research on cirrus cloud residuals.

Figure 1. Cirrus cloud formation mechanisms. Traditional cirrus forms are (1) synoptic, for example as warm air overrides cold, (2) anvil cirrus, as the outflow from convective storms and (3) formed at the cold tropopause, often in the tropics. Orographic clouds, formed from flow over terrain, are sometimes considered a type of cirrus although, unlike the other types, they are directly coupled to the surface. Contrail cirrus are an anthropogenic cloud formed by the injection of water vapor.

Figure 2. Conceptual diagram of water nucleation. Liquid water droplets form on a condensation nucleus. Ice nucleation can be divided into two broad categories: homogeneous and heterogeneous. Homogeneous freezing occurs spontaneously within an aqueous droplet which may or may not contain solutes. Heterogeneous freezing is further subdivided into multiple modes. These include (1) immersion/condensation freezing by an IN within a water capsule, (2) contact freezing when an IN makes contact with a droplet, and (3) depositional freezing of water vapor directly onto the IN surface. Less well understood modes, such as "inside out nucleation" are described in the text but not pictured here.

Figure 3. Ice nucleation mechanisms within supersaturation versus temperature space. Homogeneous freezing only occurs at low temperature and high supersaturation. Conceptual atmospheric trajectories A and B (red and green lines, respectively) pass through the various heterogeneous modes before the homogeneous freezing threshold is encountered. Trajectory A is representative of a convective storm system, where aerosol particles from the lower troposphere are subjected to water vapor near saturation levels throughout vertical transport. Trajectory B is representative of upper tropospheric particles that experience local increase in RH, for instance from a wave-induced temperature perturbation or low velocity vertical transport. This type of phase diagram has been presented previous authors, most recently by DeMott et al. [2013].

Figure 4. Ice crystal separation from interstitial aerosol using an idealized CVI inlet. In this diagram the aircraft is flying from right to left with the counterflow in the same direction. Aerosol particles (red circles) are unable to overcome the inertial barrier generated by the counterflow whereas ice crystals (light blue hexagons) can. The velocity of the crystals is reduced and the warm, dry counterflow, where red hatching denotes heaters, sublimates the ice and releases an IR. The IR is removed for analysis and excess flow is exhausted.

Figure 5. Stopping and sublimation distance as a function of ice crystal diameter calculated using a coupled fluid flow and heat transfer model that assumes spherical ice crystals. The super-100 micrometer diameter mode size of typical cirrus ice crystals

occupy the shaded region. CVI inlets are typically ~ 0.5 m in length, which corresponds to a maximum ice crystal size of < 30-50 micrometers for realistic CVI flows (dashed lines). Note that crystal sublimation is negligible prior to velocity reduction so that in traditional CVIs, these distances are additive.

Figure 6. Representative ice crystal size distributions for subvisible and two anvil cirrus clouds [Lawson et al., 2008; Davis et al., 2010]. The noted regions correspond to the size ranges that can be separated by traditional and enhanced CVI inlets, respectively (see Figure 5). Note that even with the CVI enhancements described in the text, only ice crystals smaller than ~60 – 70 micrometers diameter can be sampled.

Figure 7. Ice crystal shatter on an idealized cloud probe and a CVI inlet. Shatter is a function of aircraft speed, ice crystal size and morphology, and other properties. Crystal impaction produces artifacts by abrading aircraft and inlet material. Upon removal of condensed phase water, crystal fragments release the original IR and any scavenged gas- or particle-phase material. Artifact generation mechanisms are discussed in the text.

Figure 8. Artifacts from ice crystal impaction identified in SPMS analysis of IR. Each panel represents a different artifact generation mechanism. Altitude, temperature, and aerodynamic diameter are shown. Identification was verified by laboratory generation of particles from aircraft and inlet materials using a diamond coated tool. Panel A: stainless steel particle from crystal impaction inside the CVI inlet. Panel B: the coating from a thermistor located inside the CVI but downstream of the IR sample pickoff, demonstrating upstream travel of crystal impaction debris. Panel C: white aircraft paint from a shroud upstream of the CVI inlet, demonstrating that crystal fragments acquire material from impaction sites and can retain sufficient size to subsequently pass through the counterflow. Panel D: internal mixture of a real mineral dust IR with a small amount of gold acquired by crystal impaction inside a gold plated CVI. Panel E: sea salt particle previously adsorbed onto the CVI internal surface that was resuspended by crystal impaction. The low intensity and homogeneity of metallic signatures suggests that the adsorbed sea salt leached small amounts of metals from the stainless steel inlet. Note that in the cases of Panels D and E a signal sensitivity range of at least a factor of 200 is required to verify even the most intense artifact signatures (red color text) with certainty.

Property	Mean	Range
Altitude (km)	9.0	4.0 to 20.0
Thickness (km)	1.5	0.1 to 8.0
Concentration (L^{-1})*	30.0	10^{-4} to 10^{4}
Ice Content (g m^{-3})	0.025	10^{-4} to 1.2
Crystal Size (mm)	250	1 to 8000

Adapted from Cirrus [2000]

Table 1.

Reference	Study	Location	Season, Year	Aircraft	Ice Cloud Flights	IR Particles Analyzed	Notes	Shatter considered?
Noone et al. [1992]	ICE	Northern Europe	Fall, 1989	DLR Falcon	4 cirrostratus	IR number and size	First CVI use in cirrus.	No
Ström et al. [1994]	ICE	Northern Europe	Fall, 1989	DLR Falcon	4 cirrostratus	IR number and size	Additional discussion of bimodal IR in ICE.	No
Ström and Heintzenberg [1994]		Germany, Austria	Winter, 1992	DLR Falcon	2 glaciated	IR number only	>3000 IR/L common.	No
Heintzenberg et al. [1996]		Germany, Austria	Winter, 1992	DLR Falcon	1 glaciated	EM: 84 IRs	Mineral dust and metals.	No
Ströhm et al. [1997]		Germany, Austria	Winter, 1994	DLR Falcon	1 cirrus	IR number and size	>2500 IR/L common.	No
Petzold et al. [1998]	AEROCONTRAIL	Germany, Austria	Fall, 1996	DLR Falcon	2 contrails, 2 cirrus	EM: 380 contrail, 197 cirrus IRs	BC, metals and mineral dust.	No
Ström and Ohlsson [1998]	AEROCONTRAIL	Germany	Fall, 1996	DLR Falcon	5 contrails/cirrus	Absorbing aerosol via PSAP	Absorbing aerosol common in IR.	No
Twohy and Gandrud [1998]	SUCCESS	South, West USA	Spring, 1996	NASA DC-8	2 contrails	EM: 111 contrail	BC, metals and mineral dust.	No
Seifert et al. [2003]	INCA	Scotland, Chile	Spring, Fall, 2000	DLR Falcon	19 glaciated	IR number and size	Bimodal IR distribution.	No
Seifert et al. [2004]	INCA	Scotland, Chile	Spring, Fall, 2000	DLR Falcon	19 glaciated	IR volatility	Non-volatile IR common.	No
Cziczo et al. [2004a]	CRYSTAL-FACE	Florida, USA	Summer, 2002	NASA WB-57	12 anvil and synoptic cirrus	SPMS: 238	Mineral dust, sea salt, 1 sulfate dominated cloud.	Yes
Cziczo et al. [2004a]	CRYSTAL-FACE	Florida, USA	Summer, 2002	NASA WB-57	1 cirrus	SPMS: 127	Additional discussion of organic aerosol.	Yes
Twohy and Poellot [2005]	CRYSTAL-FACE	Florida, USA	Summer, 2002	ND Citation	14 anvil cirrus	EM: 1115	Sea salt, mineral, metals, soot.	Partial
Targino et al. [2006]	INTACC	Scandanavia	Fall, 1999	Met Office C-130	5 orographic	EM: 609	Mineral dust, sea salt, organic, metal.	Yes
Pratt et al. [2009]	ICE-L	Wyoming, USA	Fall, 2007	NCAR C-130	1 orographic	SPMS: 46	Mineral dust, mineral dust+biological.	Unknown
Froyd et al. [2010]	CRAVE	Costa Rica	Winter, 2006	NASA WB-57	4 tropopause cirrus	SPMS: 127	Sulfate, organic; inferred glasses and anhydrous salts.	Yes
Stith et al. [2011]	PACDEX	Pacific	Spring, 2007	NCAR GV	14 glaciating	EM: 4108	Combined residuals and scavenged. Biomass burning.	Yes
Baumgardner et al. [2008]	PACDEX	Pacific	Spring, 2007	NCAR GV	7 glaciated cirrus	SP2	Only black carbon measured from both IR and scavenged.	No
Cziczo et al. [2013]	CRAVE	Costa Rica	Winter, 2006	NASA WB-57	4 anvil cirrus	SPMS: 467	Mineral dust, metallic.	Yes
	TC4	Costa Rica	Summer, 2007	NASA DC-8	13 anvil and synoptic cirrus	SPMS: 438	Mineral dust, metallic, sea salt.	Yes
	MACPEX	Houston, TX	Spring, 2010	NASA WB-57	14 anvil and synoptic cirrus	EM: 433; SMPS: 330	Mineral dust, metallic, sea salt, 1 sulfate dominated cloud.	Yes

Table 2.

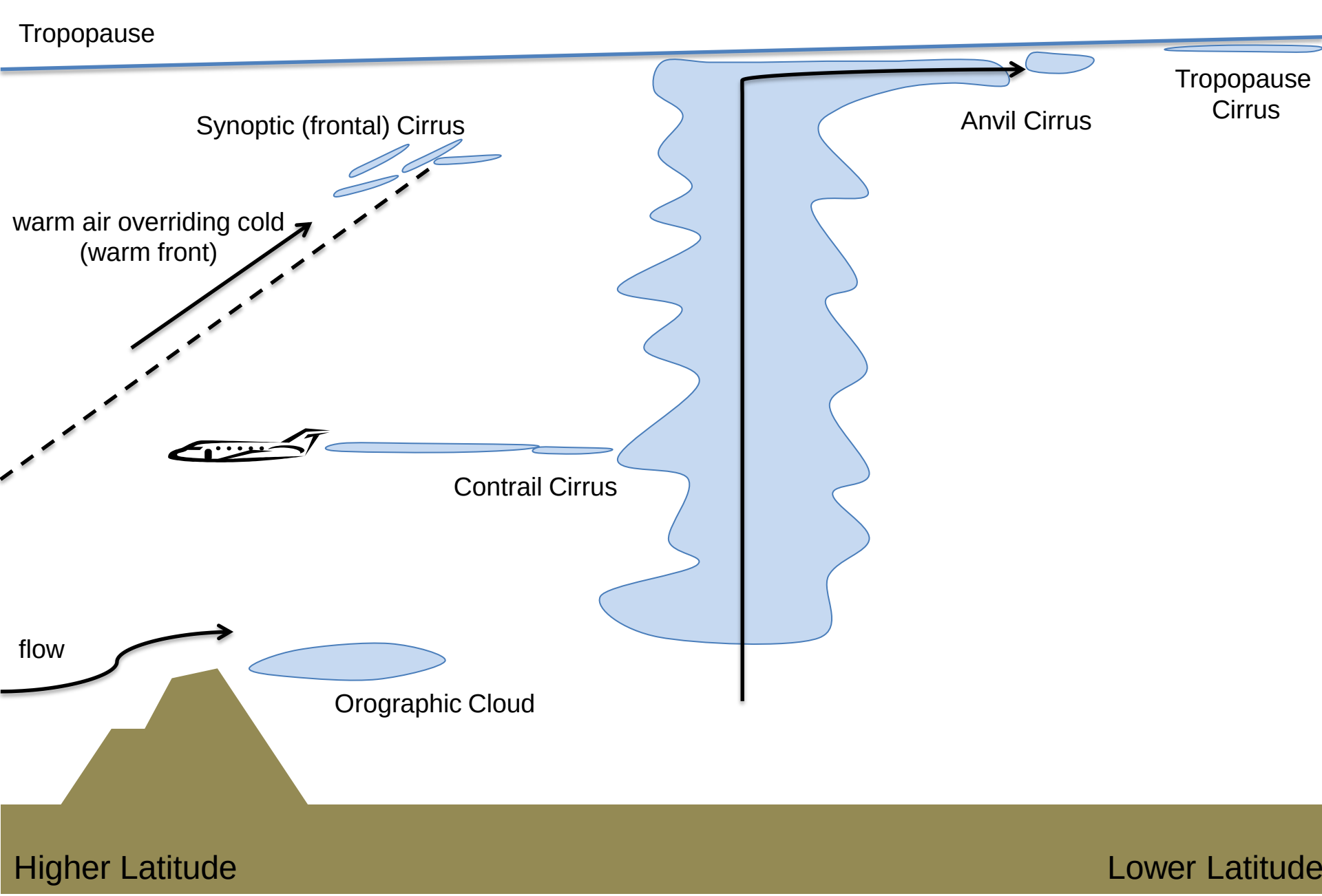
Tropopause
Synoptic (frontal) Cirrus
Anvil Cirrus
Tropopause Cirrus
warm air overriding cold (warm front)
Contrail Cirrus
flow
Orographic Cloud
Higher Latitude
Lower Latitude

Figure 1.

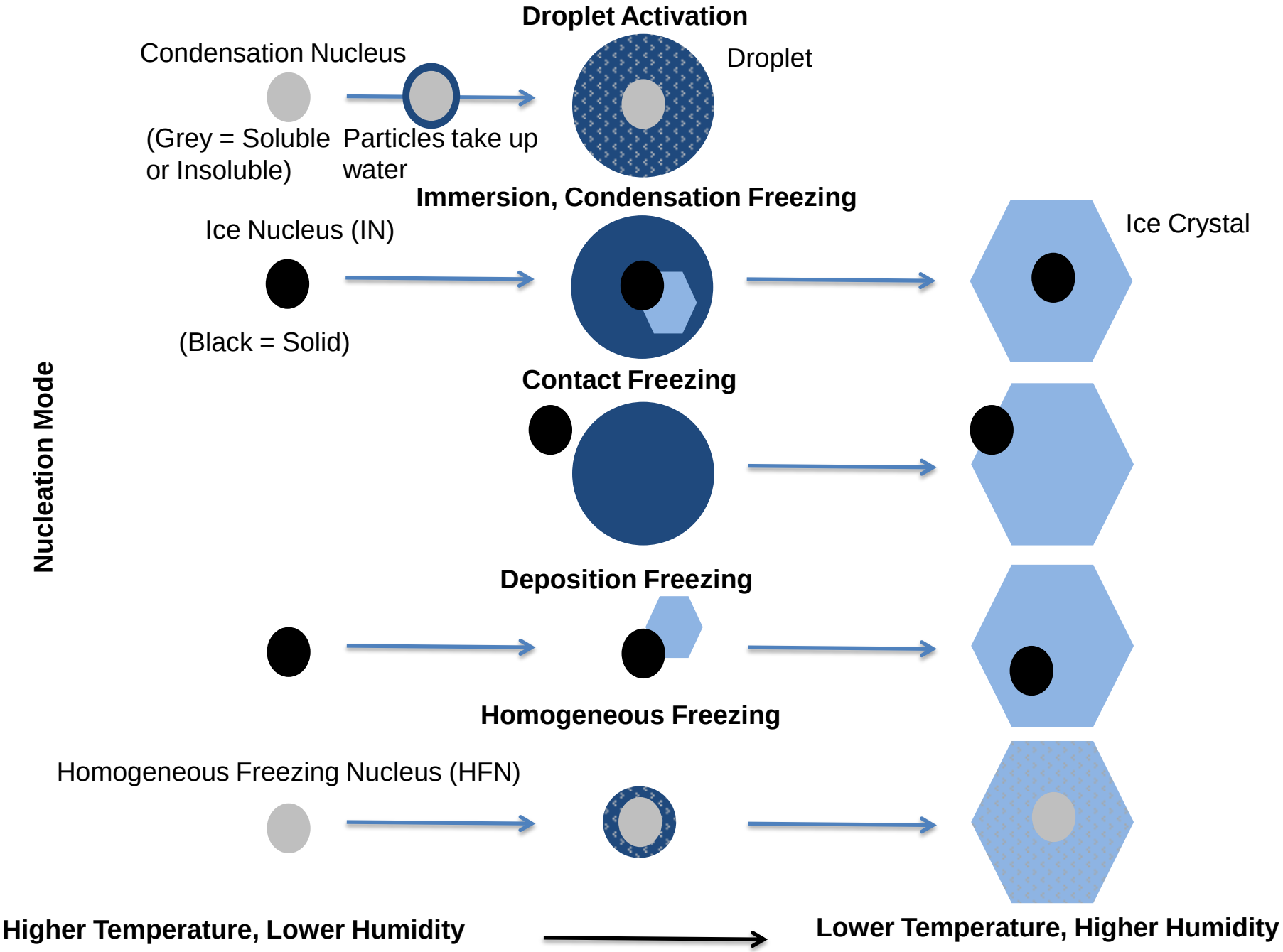
Droplet Activation
Condensation Nucleus
Droplet
(Grey = Soluble or Insoluble)
Particles take up water
Immersion, Condensation Freezing
Ice Nucleus (IN)
Ice Crystal
(Black = Solid)
Contact Freezing
Deposition Freezing
Homogeneous Freezing
Homogeneous Freezing Nucleus (HFN)
Nucleation Mode
Higher Temperature, Lower Humidity
Lower Temperature, Higher Humidity

Figure 2.

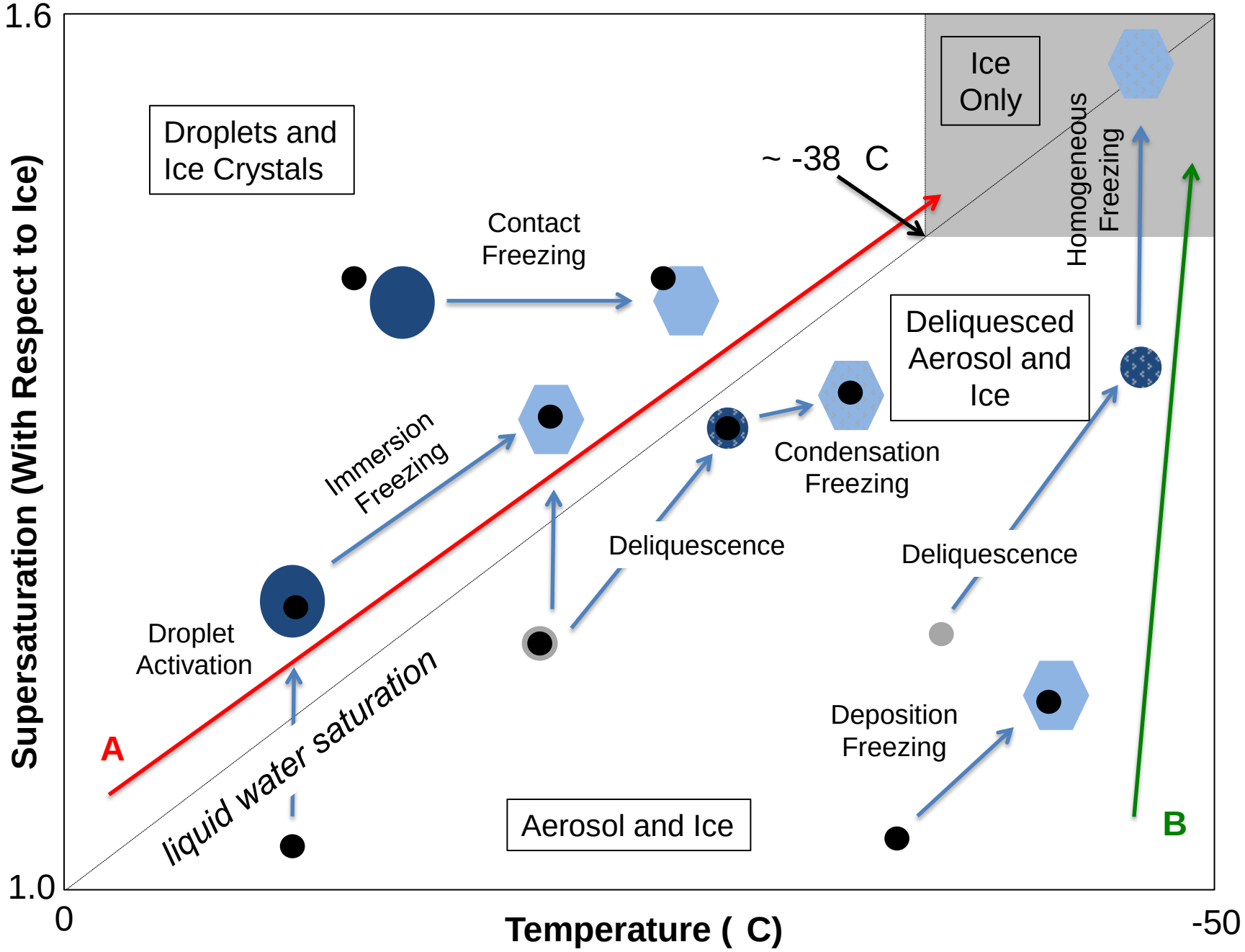
1.6
1.0
0
-50
Supersaturation (With Respect to Ice)
Temperature (C)
Droplets and Ice Crystals
Ice Only
~ -38 C
Homogeneous Freezing
Contact Freezing
Deliquesced Aerosol and Ice
Immersion Freezing
Condensation Freezing
Deliquescence
Deliquescence
Droplet Activation
A
liquid water saturation
Deposition Freezing
Aerosol and Ice
B

Figure 3.

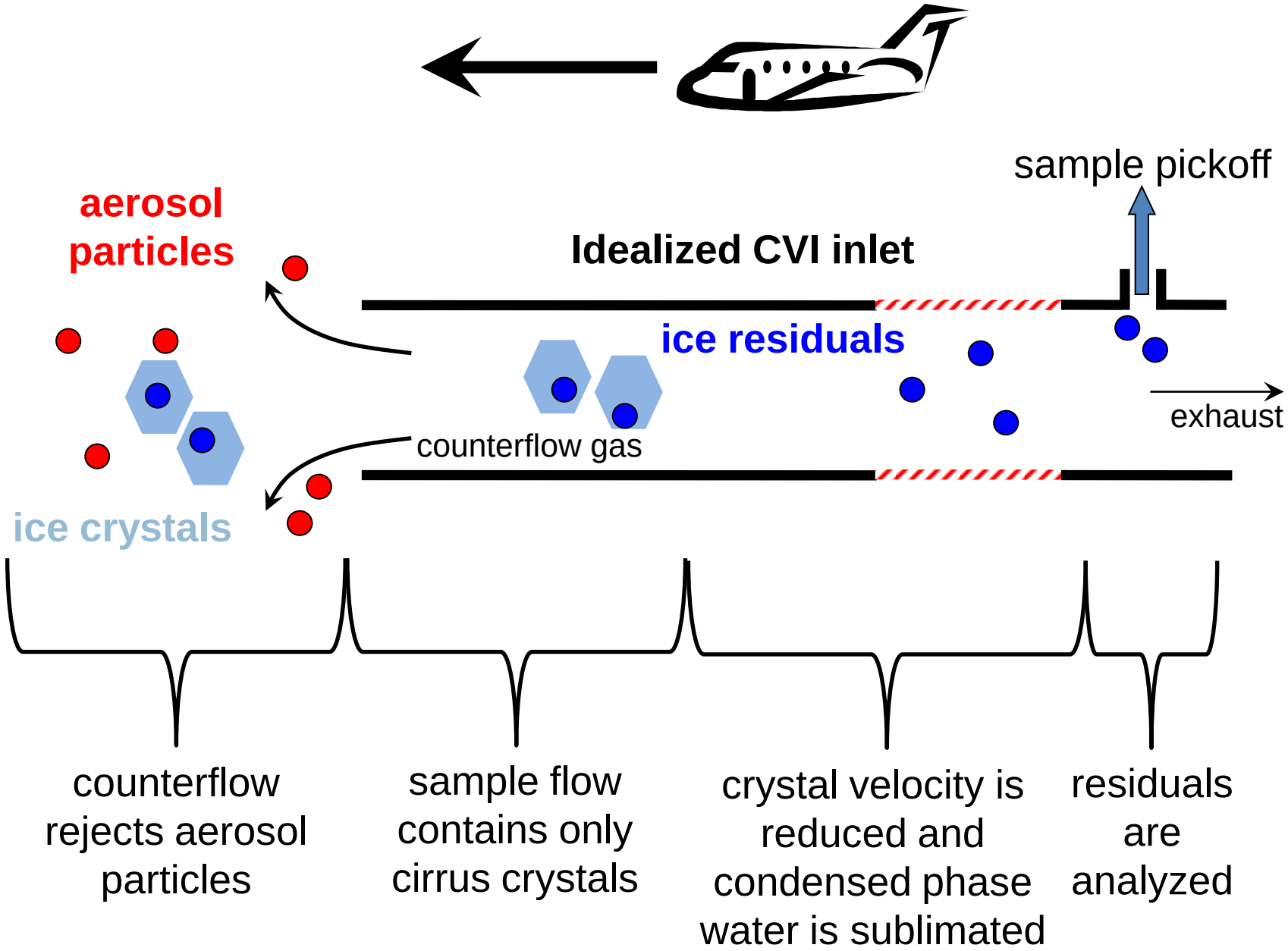
aerosol particles
Idealized CVI inlet
sample pickoff
ice residuals
exhaust
counterflow gas
ice crystals
counterflow rejects aerosol particles
sample flow contains only cirrus crystals
crystal velocity is reduced and condensed phase water is sublimated
residuals are analyzed

Figure 4.

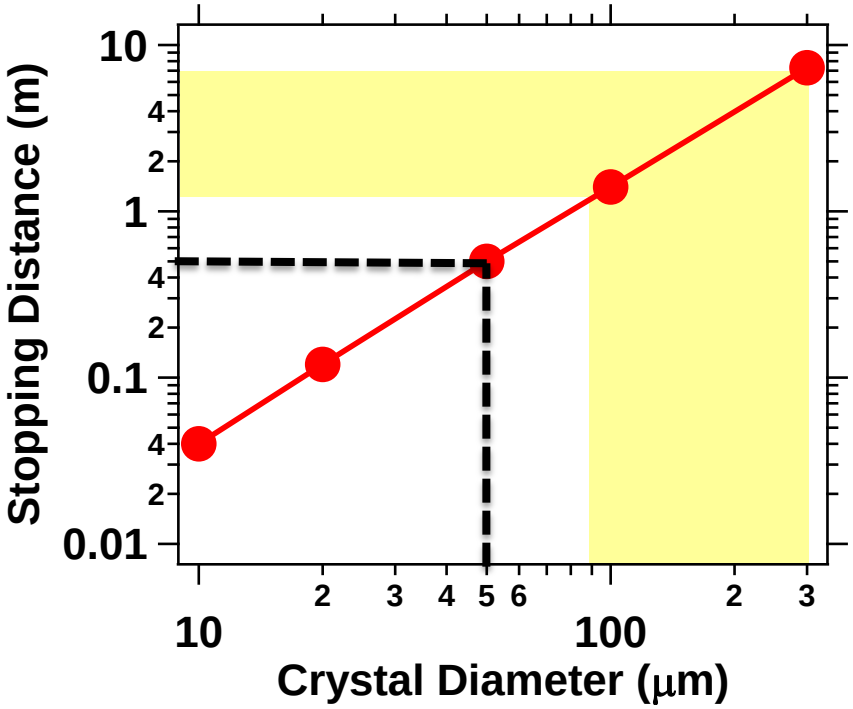
Stopping Distance (m)
10
4
2
1
4
2
0.1
4
2
0.01
10
2
3
4
5
6
100
2
3
Crystal Diameter (μm)

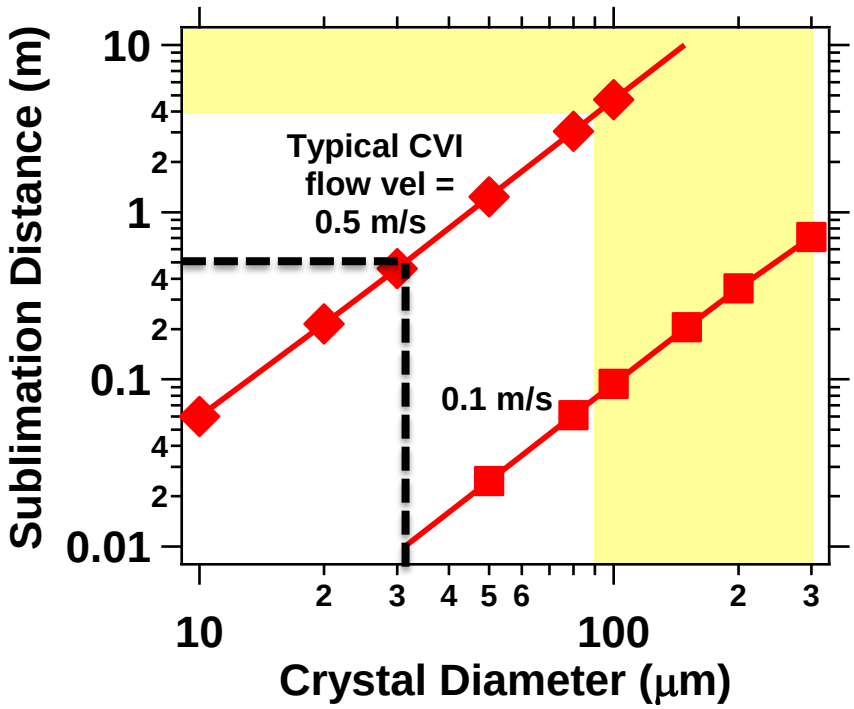
Sublimation Distance (m)
10
4
2
1
4
2
0.1
4
2
0.01
Typical CVI
flow vel =
0.5 m/s
0.1 m/s
10
2
3
4
5
6
100
2
3
Crystal Diameter (μm)

Figure 5.

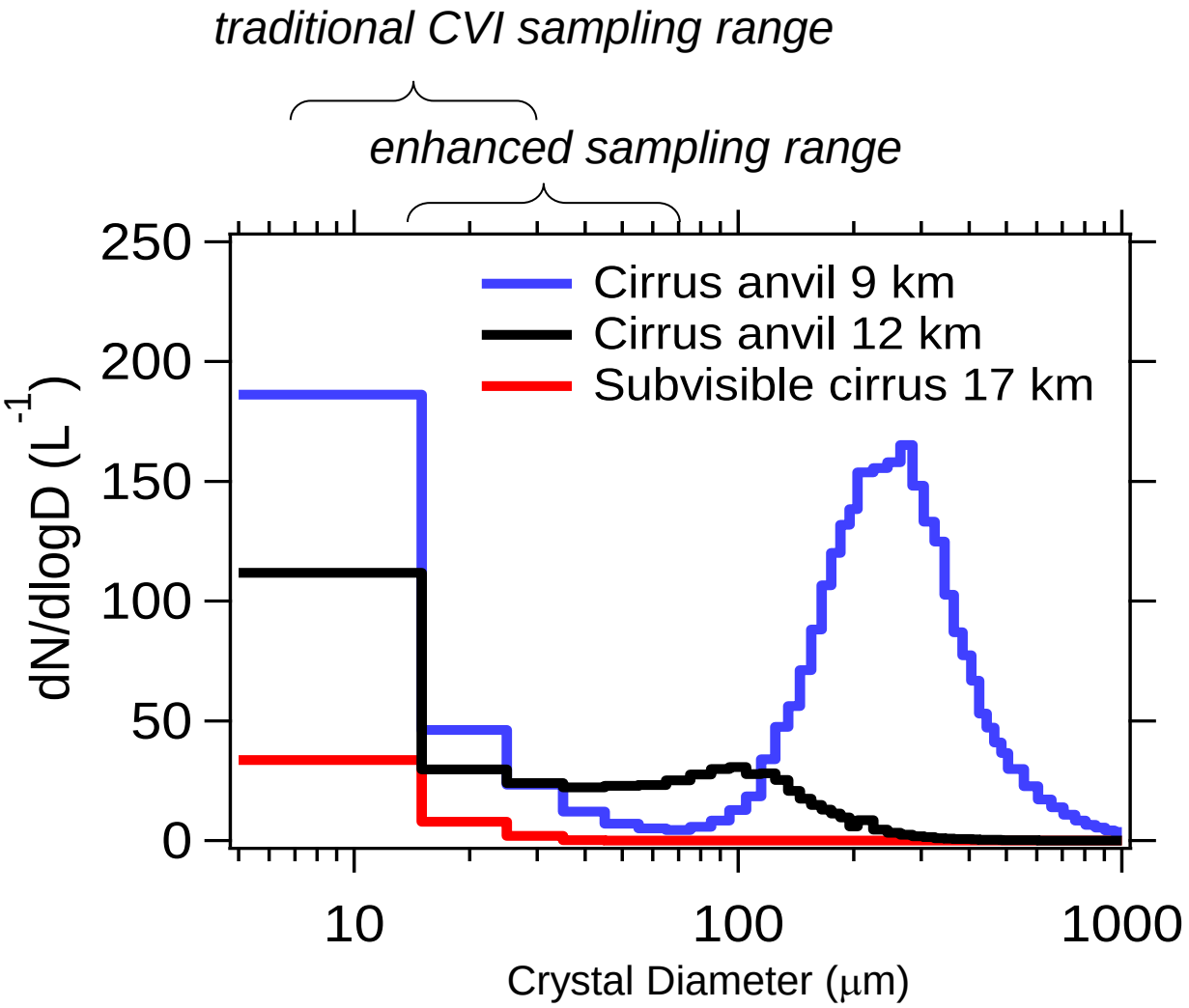
traditional CVI sampling range
enhanced sampling range
Cirrus anvil 9 km
Cirrus anvil 12 km
Subvisible cirrus 17 km
dN/dlogD (L-1)
250
200
150
100
50
0
10
100
1000
Crystal Diameter (μm)

Figure 6.

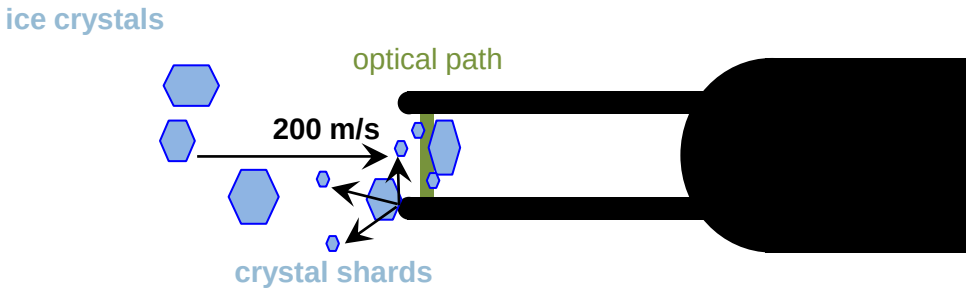

Idealized Cloud Probe

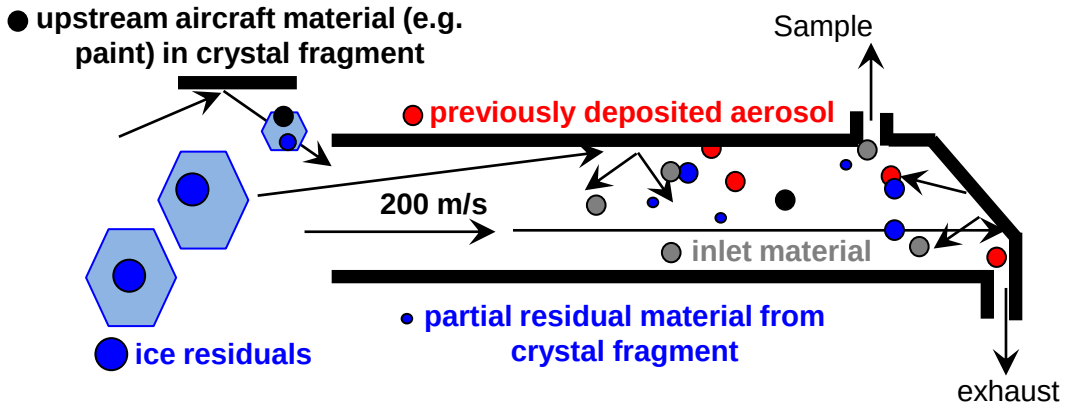

Idealized CVI Inlet

Figure 7.

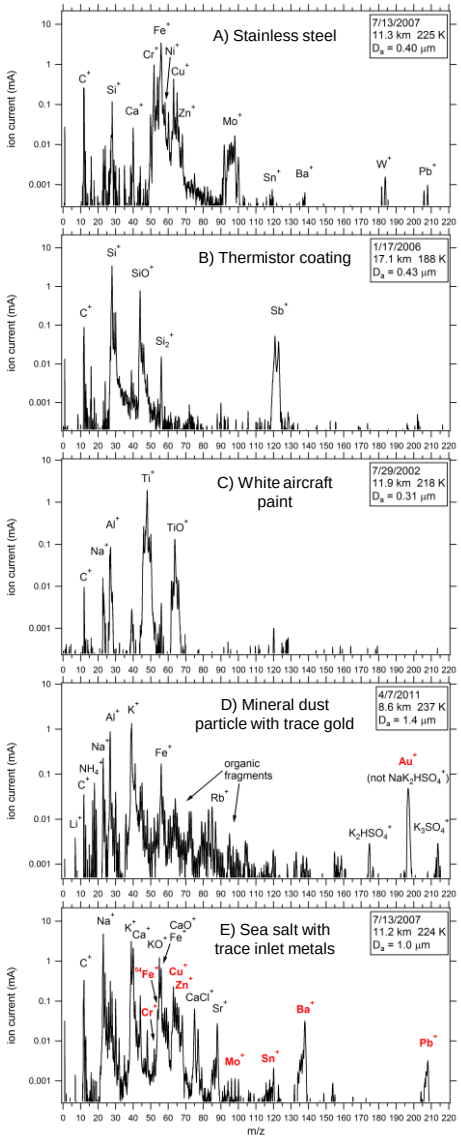
A) Stainless steel
7/13/2007
11.3 km 225 K
Da = 0.40 µm
B) Thermistor coating
1/17/2006
17.1 km 188 K
Da = 0.43 µm
C) White aircraft paint
7/29/2002
11.9 km 218 K
Da = 0.31 µm
D) Mineral dust particle with trace gold
4/7/2011
8.6 km 237 K
Da = 1.4 µm
organic fragments
Au+ (not NaK2HSO4+)
E) Sea salt with trace inlet metals
7/13/2007
11.2 km 224 K
Da = 1.0 µm
ion current (mA)
m/z

Figure 8.